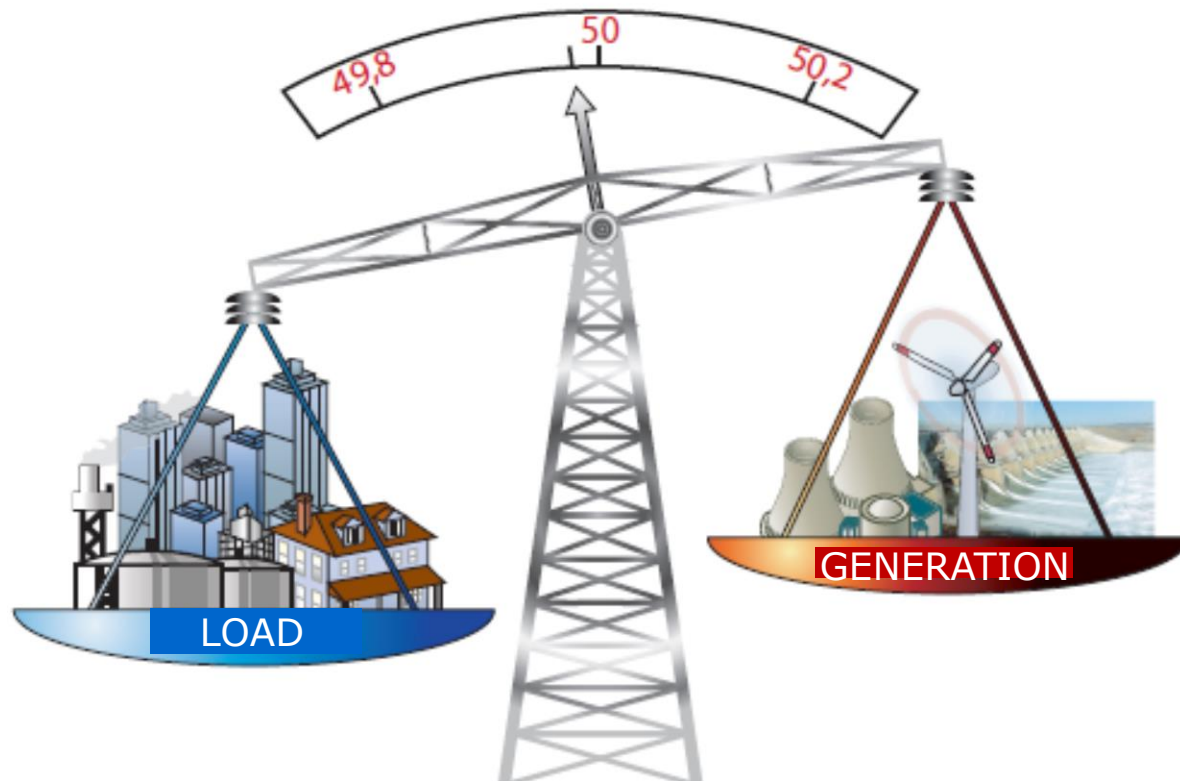

Accurate Battery Operation Modeling

Assoc. Prof. Hrvoje Pandžić

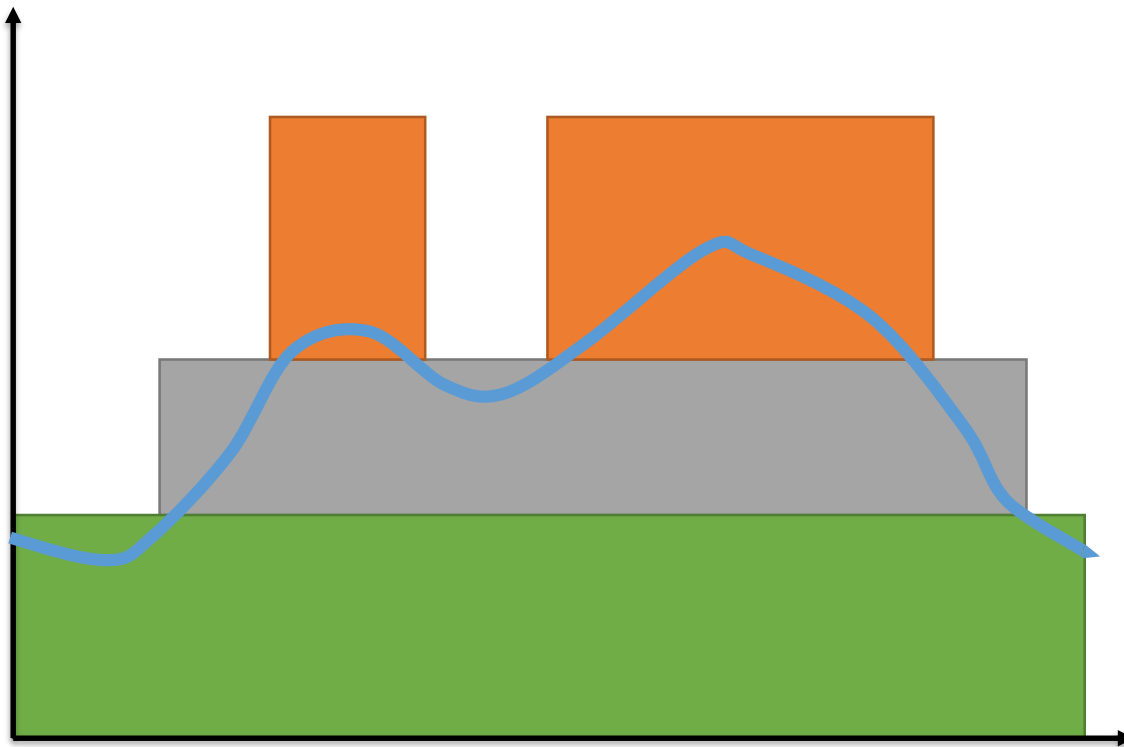
Vedran Bobanac, PhD

*Workshop on Demand Response and Energy Storage Modeling
Faculty of Electrical Engineering and Computing University of Zagreb
Zagreb, June 19, 2018*

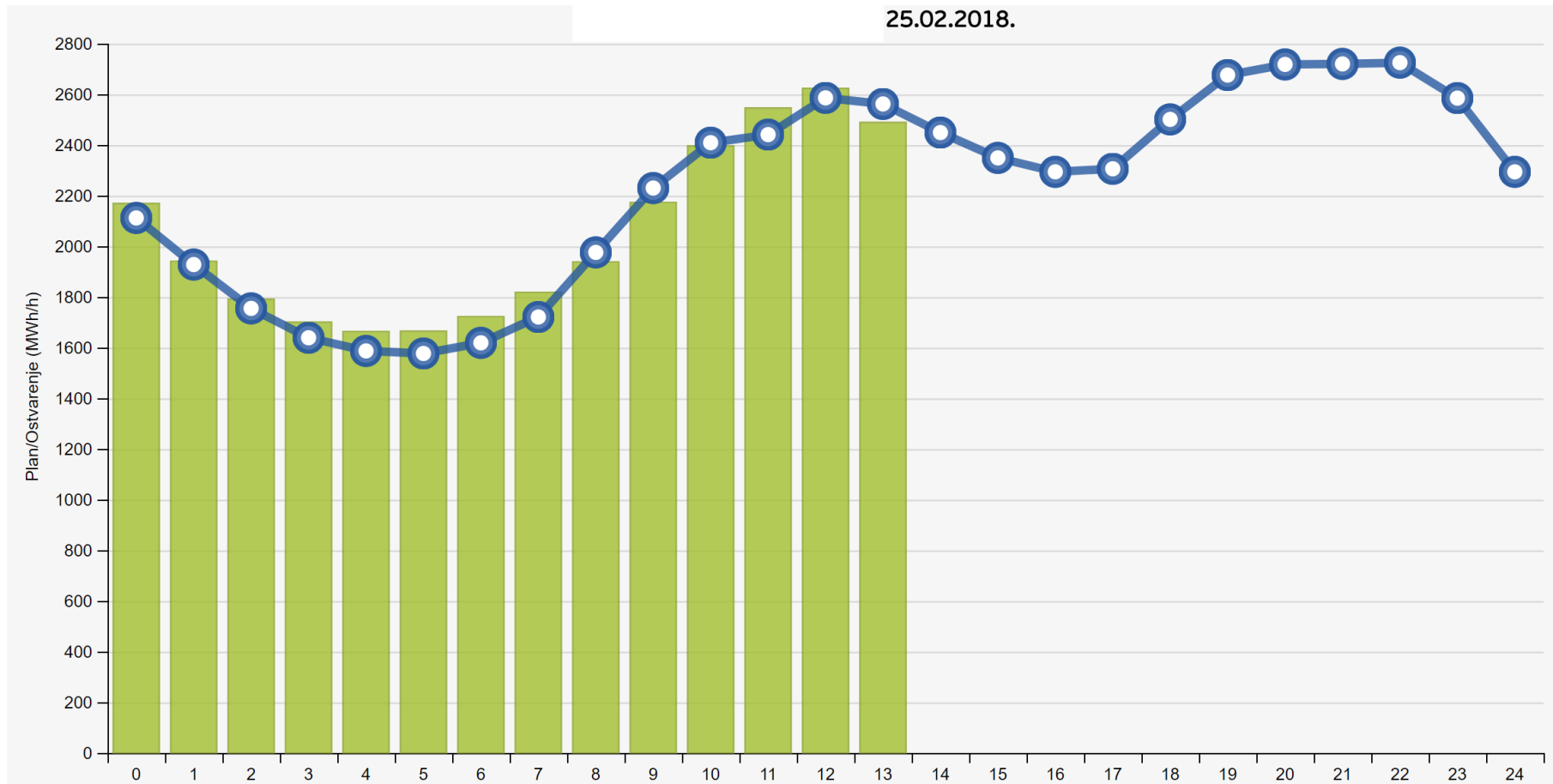
Power System



Daily Load Curve



Daily Load Curve



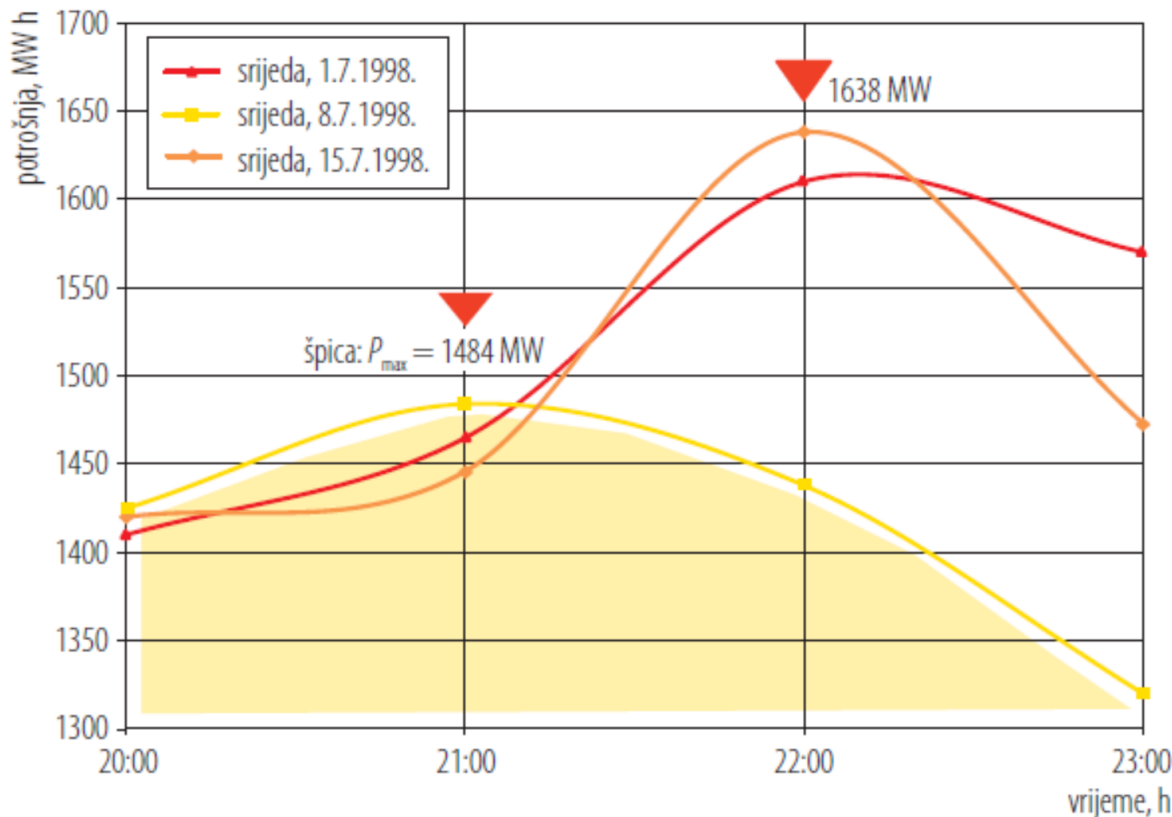


Load Forecasting

- ☐ Based on historical data
- ☐ Relatively simple task
- ☐ Error within 5%
- ☐ Temperature has the greatest influence (HVAC)
- ☐ Influence of certain specific events

Load Forecasting

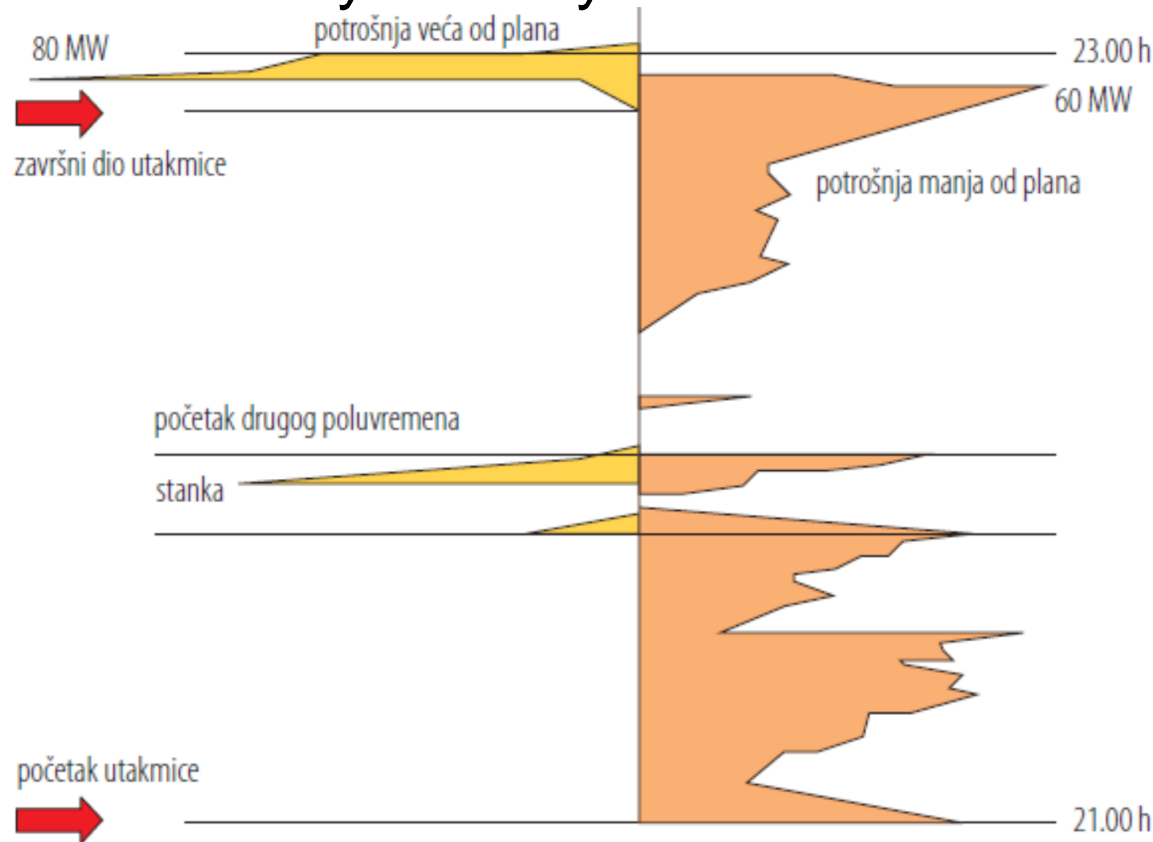
- 1998 FIFA World Cup Semi-Finals: France - Croatia, Wednesday 8th July 1998



Niko Mandić, „What connects football and power system?,” EGE 3/2008, pp. 44-50

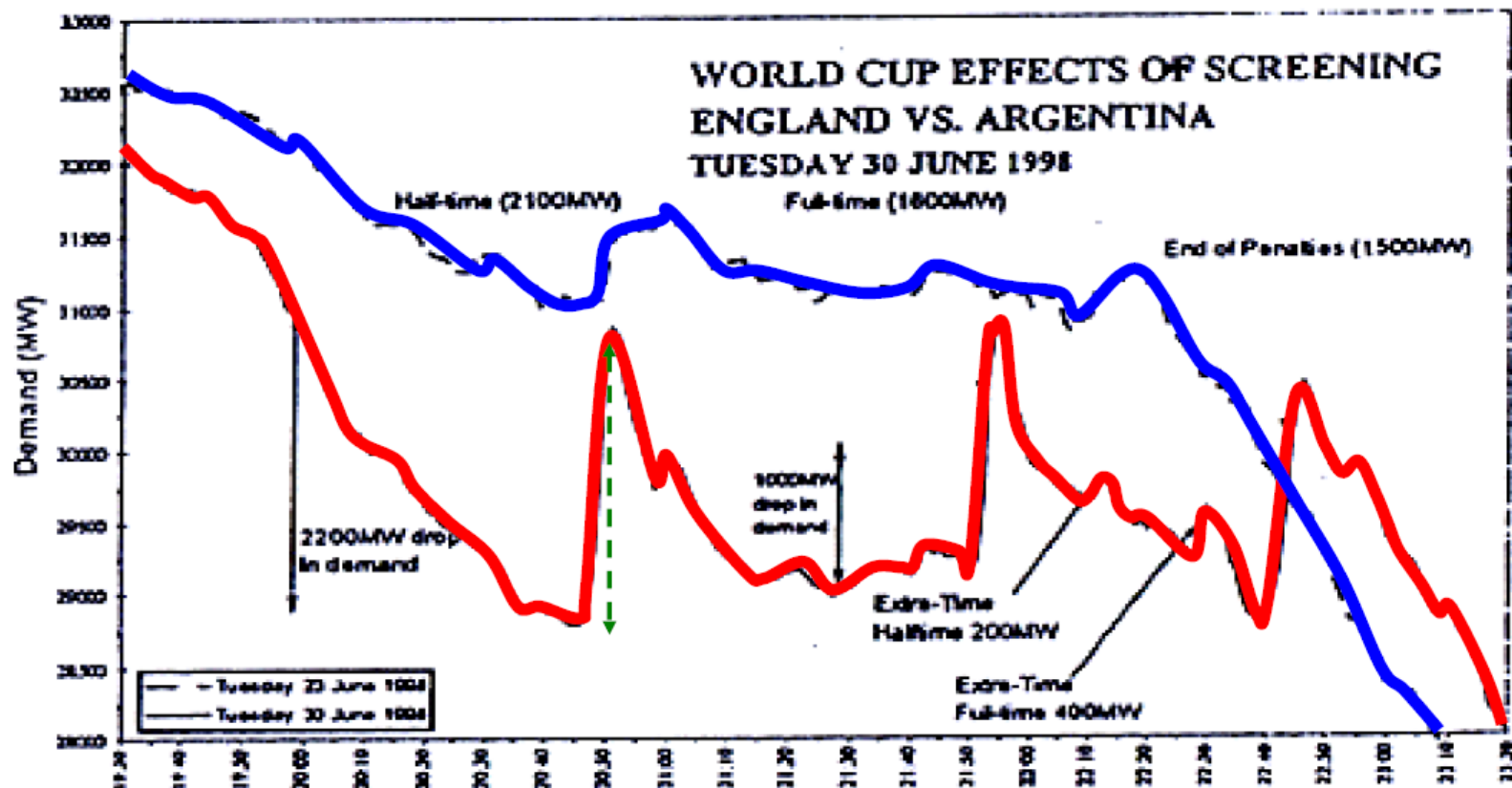
Load Forecasting

- 1998 FIFA World Cup Semi-Finals: France - Croatia, Wednesday 8th July 1998



Niko Mandić, „What connects football and power system?,” EGE 3/2008, pp. 44-50

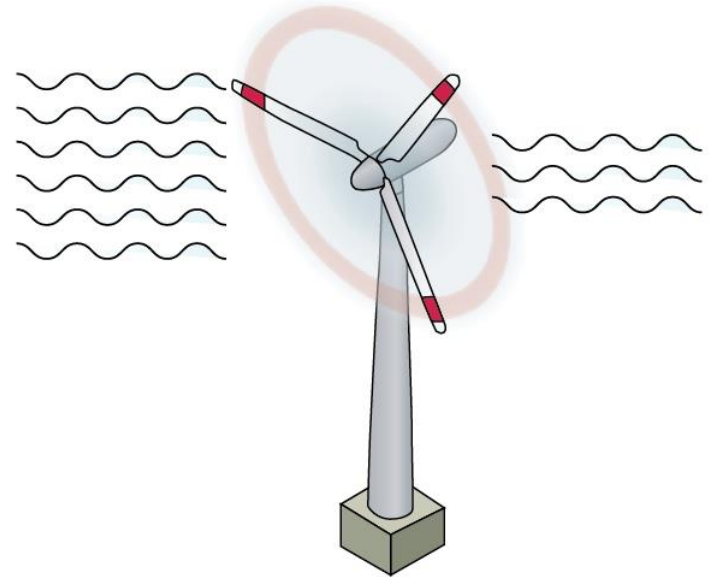
Load Forecasting



Ilustracija 5 : Detalj originalnog zapisa NG (Engleska) potrošnje električne energije za vrijeme nogometne utakmice Engleska-Argentina 30.06 1998. godine u vremenu 19:10 do 23:30. Rezolucija vremenske ose je 10 minuta. Plavi grafikon prikazuje potrošnju srijeda 23.06. 1998. godine crvenom bojom grafikon potrošnje srijeda 30.06. 1998.godine sedam dana kasnije.

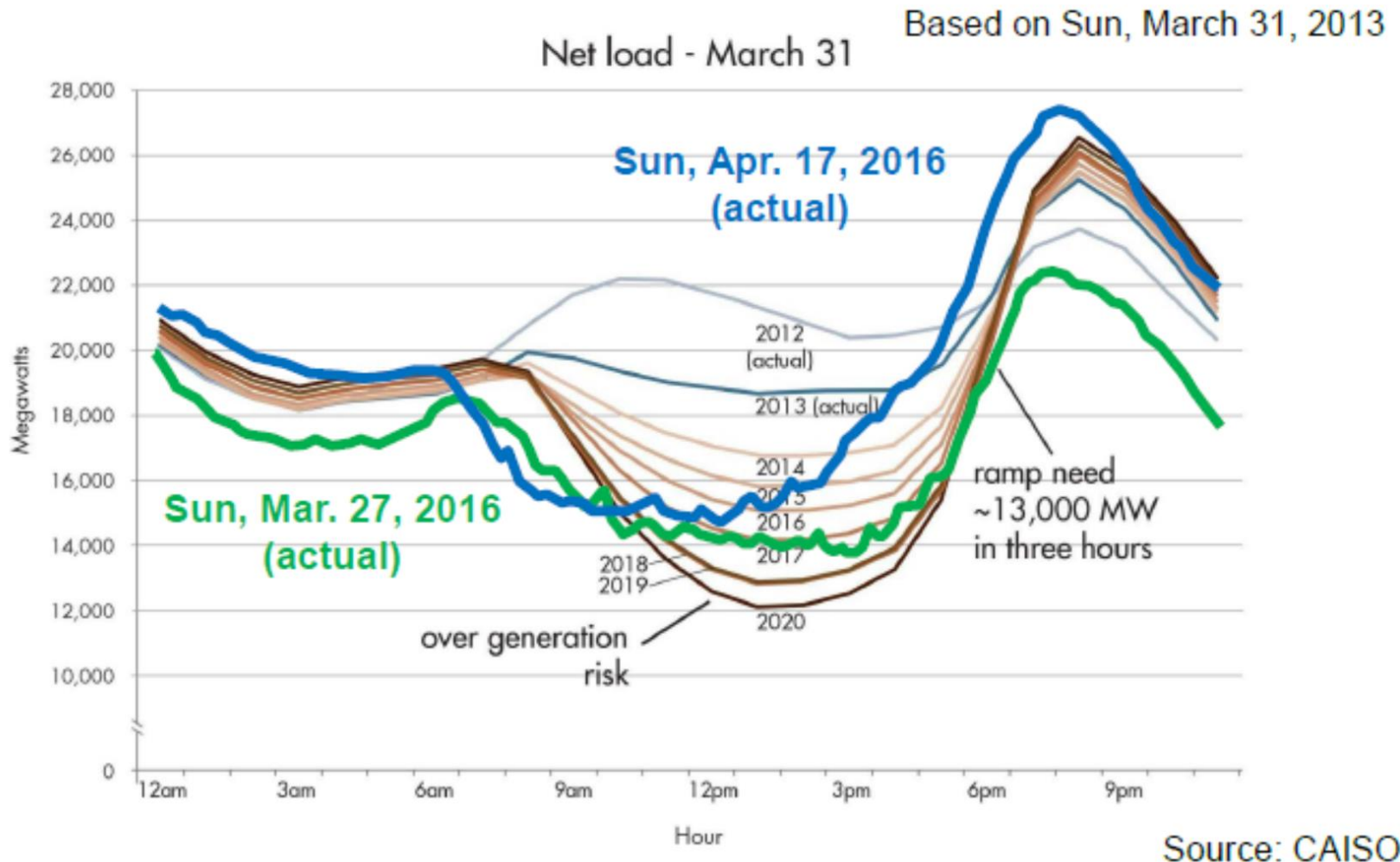
Renewable Energy Sources (RES)

- ❑ Wind energy is the most popular renewable energy source
- ❑ Wind power capacity of 744 MW is expected to be achieved within a few years
- ❑ Wind power capacity of 421 MW is already in operation
- ❑ Problematic location
- ❑ Production factor around 25%





Renewable Energy Sources



Potential Solutions

Technology	Congestion	Electricity production	Reserve provision	Positive impact on emissions
FACTS devices				
Gas power plants				
Grid reconfiguration				
Energy storage				

Potential Solutions

Technology	Congestion	Electricity production	Reserve provision	Positive impact on emissions
FACTS devices	+	-	-	-/+
Gas power plants	-	+	+	-
Grid reconfiguration	+	-	-	-/+
Energy storage	+	-/+	+	-/+

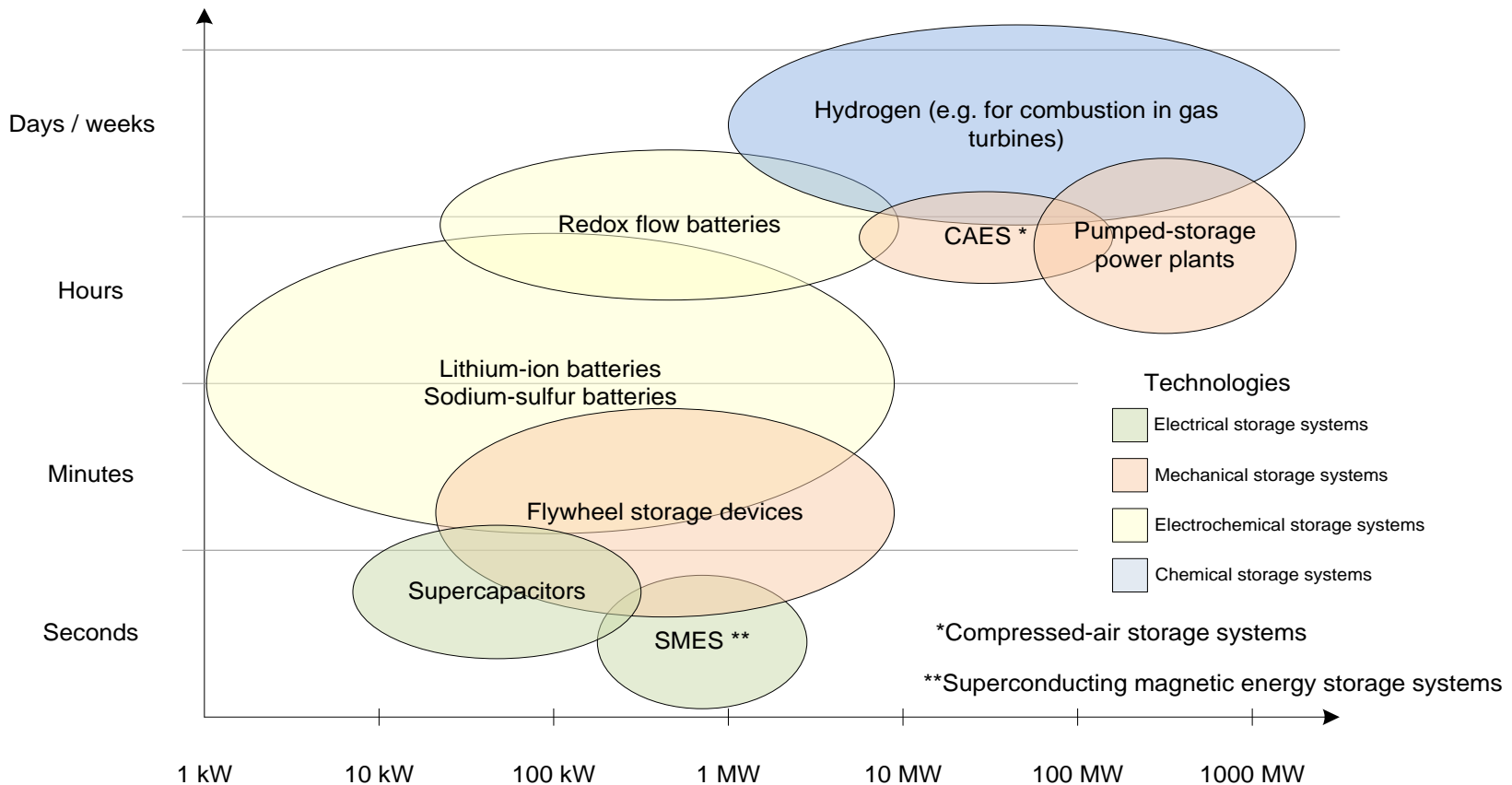
Energy Storage in Power Systems

□ Benefits:

- Levelling of the load curve
- Ancillary services (frequency containment reserve – “primary reserve”, frequency restoration reserve – “secondary reserve”, replacement reserve – “tertiary reserve” and voltage stability)
- Reduction of congestion
- Greater utilization of wind and solar energy
- More cost-effective operation of the system (less fuel, less power plant cycling, ...)
- Transition from the preventive to the corrective N-1 security operation

Energy Storage Technologies

Energy Storage Systems by Duration and Power





Energy Storage in the World

- ❑ 27 MW during 15 min NiCd – Fairbanks, AL (2003)
 - ❑ 20 MW during 15 min flywheel – Stephentown, NY (2011)
 - ❑ 32 MW during 15 min Li-Ion – Laurel Mountain, WV (2011)
 - ❑ 36 MW during 40 min Lead Acid – Notrees, TX (2012)
 - ❑ 8 MW during 4 h Li-Ion – Tehachapi, CA (2014)
 - ❑ 25 MW during 3 h Flow bat. – Modesto, CA (2014)
 - ❑ 5 MW during 1 h Li-Ion – Schwering, Germany (2014)
 - ❑ 6 MW during 1:40 h Li-ion – Leighton Buzzard, UK (2014)
-
- ❑ Interactive map available at <http://www.energystorageexchange.org/projects>

Energy Storage in Italy

Power Intensive

- Mission: increase safety of grid
- Total Power: **≈ 40 MW**
- Solutions: Li-Ion, Zebra, Flow, Supercaps
- Number of sites: **2**
- Investment Size: 93 €mln;

PHASE I: 16 MW Storage Lab

Site 1 Codrongianos

- Total Power: **≈ 9,15 MW**
- Status: operational **≈ 5,4 MW**
in commissioning **≈ 2,1 MW**
under construction **≈ 0,4 MW**
procurement initiated **≈ 1,25 MW**

Site 2 Ciminna

- Total Power: **≈ 6,8 MW**
- Status: operational **≈ 5,1 MW**
under construction **≈ 0,45 MW**
tender to be submitted **≈ 1,25 MW**

PHASE II: 24 MW

Casuzze and Codrongianos: *to be initiated*

Energy Intensive

- Mission : reduce grid congestions
- Total Power: **≈ 35 MW**
- Solution: NaS Sodium Sulfur
- Number of sites: **3**
- Investment Size: 160 €mln;

Site 1: Ginestra

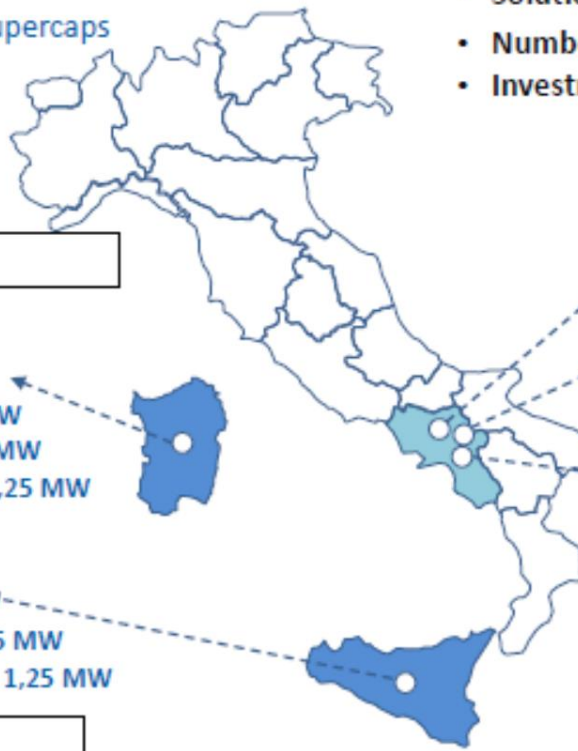
- Total Capacity: **≈ 12 MW**
- Status: operational

Site 2 Flumeri

- Total Capacity: **≈ 12 MW**
- Status: operational

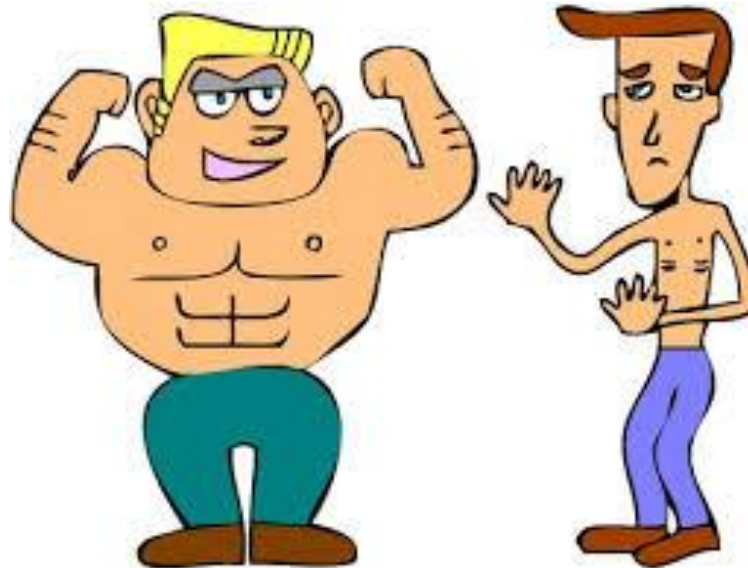
Site 3 Scampitella

- Total Capacity: **≈ 10.8 MW**
- Status: operational



Large-scale Energy Storage Models

- Price-maker vs. price-taker



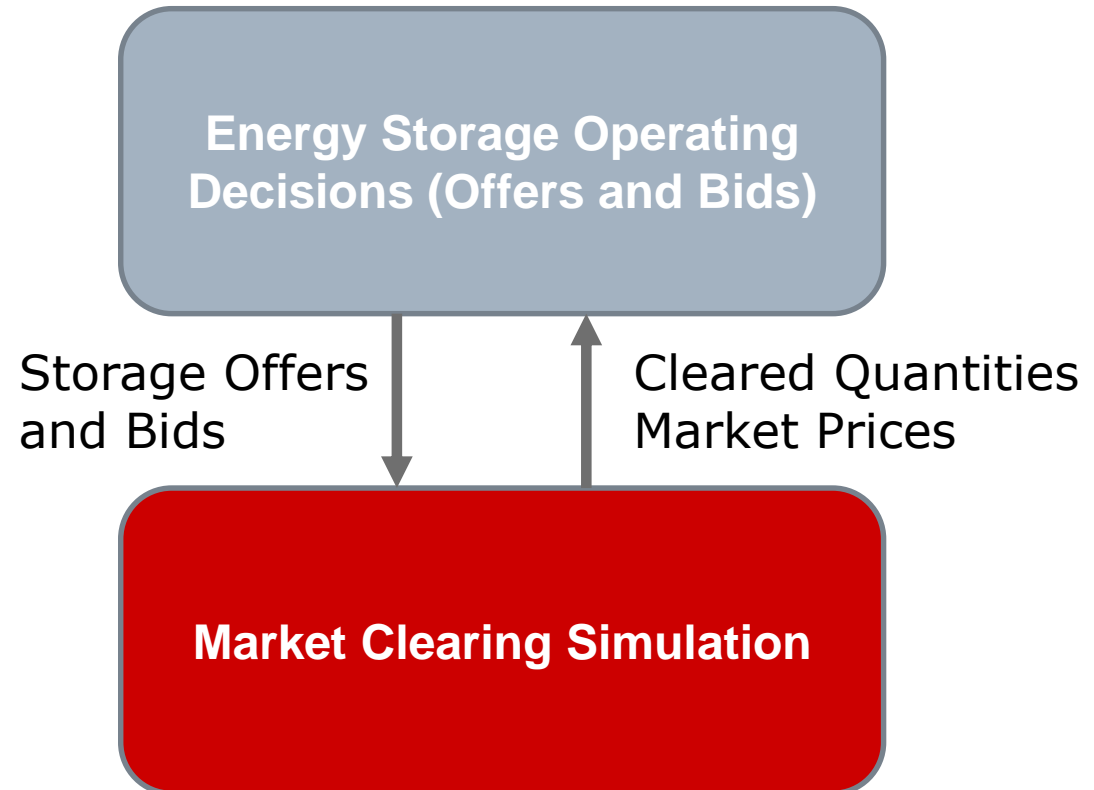
Energy Storage in the Day-Ahead Market

- Prices at CROPEX-u on Monday, February 26th 2018 (Eur/MWh)

Hour	Price	Hour	Price	Hour	Price
1	40,12	9	71,77	17	64,23
2	42,40	10	72,03	18	70,49
3	42,32	11	64,39	19	81,21
4	40,03	12	59,28	20	76,01
5	39,97	13	53,08	21	59,95
6	43,05	14	54,51	22	57,63
7	56,45	15	53,07	23	45,00
8	77,53	16	59,00	24	45,63

Large-scale Energy Storage Models

- ❑ Energy storage does not want to influence market prices
- ❑ Limited profitability when acting only in energy market





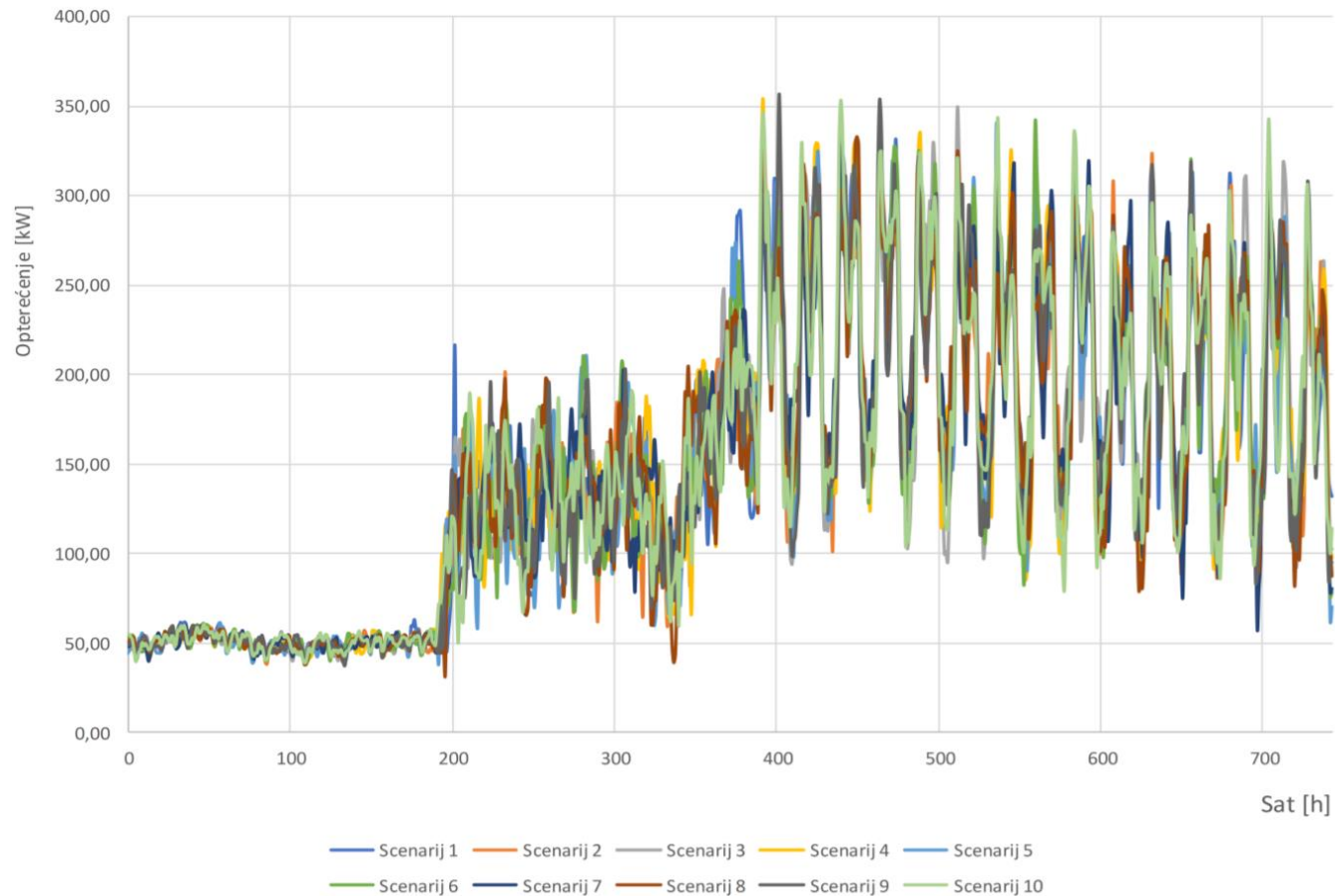
Electricity Bill Components

- ☐ Energy payment (high and low tariff)
- ☐ Distribution and transmission network charge
- ☐ Charge for meter-reading
- ☐ Charge for incentivizing RES

- ☐ Power factor charge
- ☐ Capacity charge

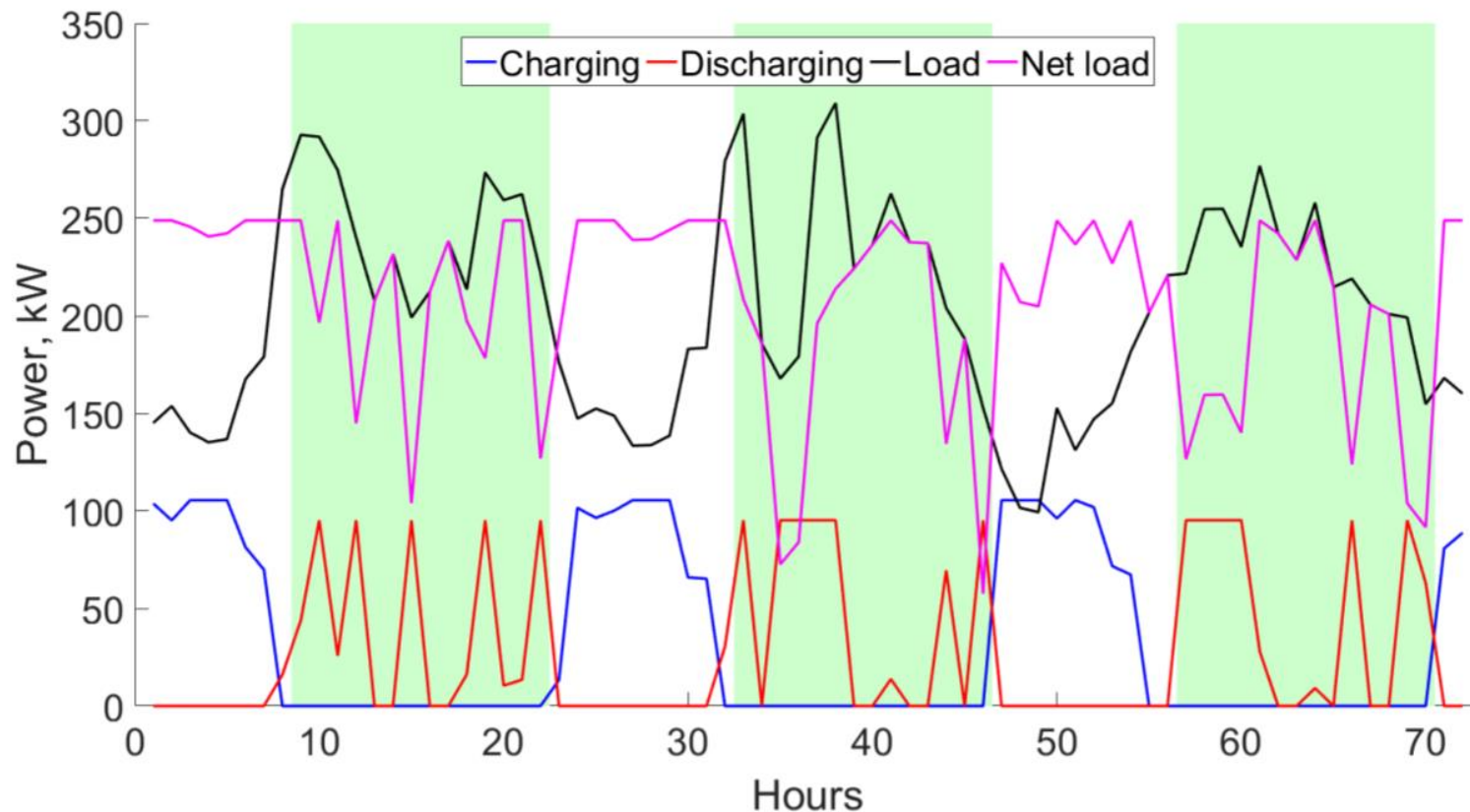
Load Diagram

- Energy storage can reduce the cost of electricity supply



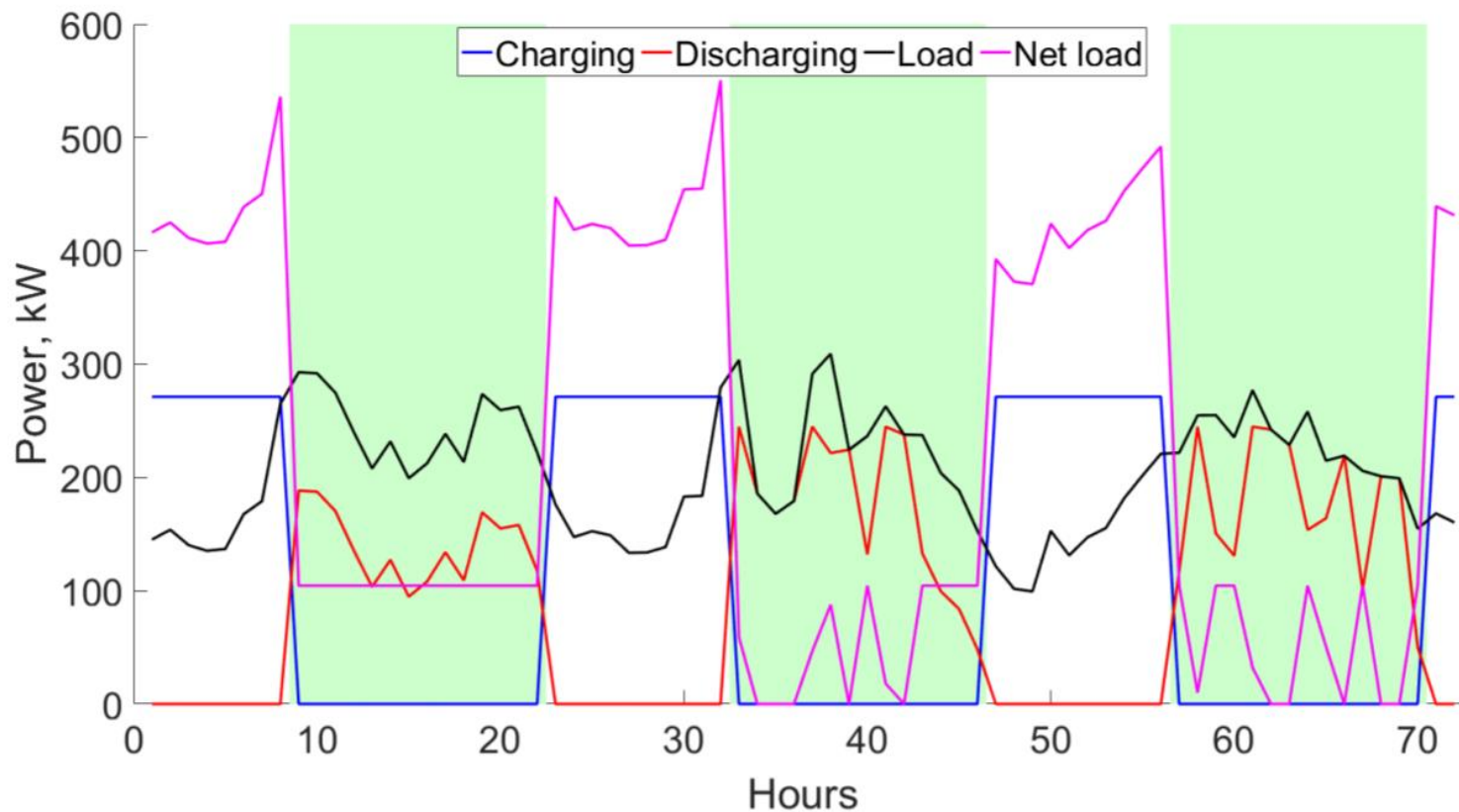
Storage Charging Profiles

- Reduced peak load payments and energy payments



Storage Charging Profiles

- Reduced peak load payments and energy payments





Batteries

- ❑ Battery is a device that converts chemical energy of its active materials directly into electrical energy through an electrochemical redox reaction
- ❑ In case of rechargeable batteries, the process is reversible
- ❑ Batteries have an efficient energy conversion since they use electrochemical process to convert chemical energy into electricity
- ❑ Although the term battery is often used, the basic unit in which the reaction occurs is known as battery cell
- ❑ Battery consists of multiple cells connected in series and parallel, depending on the desired voltage and capacity

Near-Optimal Method for Siting and Sizing of Distributed Storage in a Transmission Network

Hrvoje Pandžić, *Member, IEEE*, Yishen Wang, *Student Member, IEEE*, Ting Qiu, *Student Member, IEEE*, Yury Dvorkin, *Student Member, IEEE*, and Daniel S. Kirschen, *Fellow, IEEE*

Abstract—Energy storage can alleviate the problems that the uncertainty and variability associated with renewable energy sources such as wind and solar create in power systems. Besides applications such as frequency control, temporal arbitrage or the provision of reserve, where the location of storage is not particularly relevant, distributed storage could also be used to alleviate congestion in the transmission network. In such cases, the siting and sizing of this distributed storage is of crucial importance to its cost-effectiveness. This paper describes a three-stage planning procedure to identify the optimal locations and parameters of distributed storage units. In the first stage, the optimal storage locations and parameters are determined for each day of the year individually. In the second stage, a number of storage units is available at the locations that were identified as being optimal in the first

to alleviate congestion or otherwise enhance transmission capacity, the siting and sizing of the devices determines their usefulness and hence their cost-effectiveness.

This paper proposes a framework for optimizing the location as well as the power and energy ratings of storage units distributed across a transmission network. Because they are distributed, these storage devices can perform a spatiotemporal arbitrage that alleviates network congestion and wind spillage, thus reducing the cost of producing energy using conventional generating units. Optimizing their location and size involves balancing the operational benefit that they provide against the cost of their deployment.

Batteries in Transmission Systems

98

22

Enhanced Security-Constrained OPF With Distributed Battery Energy Storage

Yunfeng Wen, *Student Member, IEEE*, Chuangxin Guo, *Member, IEEE*, Daniel S. Kirschen, *Fellow, IEEE*,
and Shufeng Dong

Abstract—This paper discusses how fast-response distributed battery energy storage could be used to implement post-contingency corrective control actions. Immediately after a contingency, the injections of distributed batteries could be adjusted to alleviate overloads and reduce flows below their short-term emergency rating. This ensures that the post-contingency system remains stable until the operator has redispatched the generation. Implementing this form of corrective control would allow operators to take advantage of the difference between the short- and long-term ratings of the lines and would therefore increase the available transmission capacity. This problem is formulated as a two-stage, enhanced security-constrained OPF problem, in which the first-stage optimizes the pre-contingency generation dispatch, while the second-stage minimizes the corrective actions for each contingency. Case studies based on a six-bus test system and on the IEEE 118-bus system show that the proposed method can effectively reduce the peak load on the transmission lines and on the generators at the locations that were identified as the most vulnerable.

n Index to the set of load buses.
 N_C Set of contingencies.
 N_D Set of load buses.
 N_G Set of generators.
 N_L Set of transmission lines.
 N_S Set of batteries.
 N_Z Set of segments of the piecewise linear generator cost function.

Parameters:

IEEE TRANSACTIONS ON POWER SYSTEMS, VOL. 30, NO. 5, SEPTEMBER 2015
IEEE TRANSACTIONS ON POWER SYSTEMS, VOL. 30, NO. 1, JANUARY 2015

Enhanced Security-Constrained Unit Commitment With Emerging Utility-Scale Energy Storage

Yunfeng Wen, *Member, IEEE*, Chuangxin Guo, *Senior Member, IEEE*, Hrvoje Pandžić, *Member, IEEE*, and Daniel S. Kirschen, *Fellow, IEEE*

Y 2015

Abstract—We introduce emerging utility-scale energy storage (e.g., batteries) as part of the set of control measures in a corrective form of the security-constrained unit commitment (SCUC) problem. This enhanced SCUC (ESCUC) leverages utility-scale energy storage for multiple applications. In the base case, the storage units are optimally charged and discharged to realize economic operation. Immediately following a contingency, the injections of storage units are adjusted almost instantly to alleviate short-term emergency overloads, thereby avoiding potential cascading outages and giving slow ramping generating units time to adjust their output. The ESCUC is a large two-stage mixed-integer programming problem. A Benders decomposition has been developed to solve this problem. In order to achieve computational tractability, we present several acceleration techniques to improve

 J, K, L, T

Sets of cost curve segments, contingencies, lines, and time intervals.

 $G(b), S(b), L(b)$

Sets of generators, storage units, and load demands located at bus b .

B. Variables

 E_{mt}^0, E_{mt}^k

Energy stored in storage unit m at hour t for the base case and the k th contingency [MWh].

 I_{it}

On/off status of generator i at hour t .

 I_{i0}

Initial commitment status of generator i .

 I_{ij}

Parameters of the piecewise linear generator

Batteries in Transmission Systems

IEEE TRANSACTIONS ON SUSTAINABLE ENERGY, VOL. 6, NO. 1, JANUARY 2015

TRANSACTIONS ON POWER SYSTEMS, VOL. 31, NO. 1, JANUARY 2016

Coordinated Operational Planning for Wind Farm With Battery Energy Storage System

Fengji Luo, *Member, IEEE*, Ke Meng, *Member, IEEE*, Zhao Yang Dong, *Senior Member, IEEE*, Yu Zheng, *Student Member, IEEE*, Yingying Chen, *Student Member, IEEE*, and Kit Po Wong, *Fellow, IEEE*

Abstract—This paper proposes a coordinated operational dispatch scheme for a wind farm with a battery energy storage system (BESS). The main advantages of the proposed dispatch scheme are that it can reduce the impacts of wind power forecast errors while prolonging the lifetime of BESS. The scheme starts from the planning stage, where a BESS capacity determination method is proposed to compute the optimal power capacity and energy capacity of BESS based on historical wind power data; and then, at the operation stage, a flexible short-term BESS-wind farm dispatch scheme is proposed based on the forecasted wind power generation scenarios. Three case studies are provided to validate the performance of the proposed method. The results show that the proposed scheme can largely improve the wind farm dispatchability.

at t to a
teger programming
developed to solve this problem
tractability, we present several acceleration

 P_{ref}^t
 P_{BESS}^t
 P_{WF}^t
 $P_{\text{BESS}}^{\text{Chr,Max}}, P_{\text{BESS}}^{\text{Dis,Max}}$
 SOC^t
 $\text{SOC}^{\text{Min}}, \text{SOC}^{\text{Max}}$
 E_{BESS}^t
 E_{BESS}^r

Referenced power output of wind farm at time t (MW).

Power output of BESS at time t (MW).

Total power output of wind farm at time t (MW).

Maximum charge and discharge power limit of BESS (MW).

State-of-the-charge (SOC) of BESS at time t .

Lower and upper SOC limit of BESS.

Energy stored in BESS at time t (MWh).

Rated energy capacity of BESS (MWh).

253

2015

Batteries in Transmission Systems

IEEE TRANSACTIONS ON SUSTAINABLE ENERGY, VOL. 8, NO. 3, JULY 2017

IEEE TRANSACTIONS ON SUSTAINABLE ENERGY

1140

Coordinated Control Strategy of a Battery Energy Storage System to Support a Wind Power Plant Providing Multi-Timescale Frequency Ancillary Services

Jin Tan, Member, IEEE, and Yingchen Zhang, Senior Member, IEEE

53

2015

Abstract—With increasing penetrations of wind generation on electric grids, wind power plants (WPPs) are encouraged to provide frequency ancillary services (FAS); however, it is a challenge to ensure that variable wind generation can reliably provide these ancillary services. This paper proposes using a battery energy storage system (BESS) to ensure the WPPs' commitment to FAS. This method also focuses on reducing the BESS's size and extending its lifetime. In this paper, a state-machine-based coordinated control strategy is developed to utilize a BESS to support the obliged FAS of a WPP (including both primary and secondary frequency control). This method takes into account the operational constraints of the WPP (e.g., real-time reserve) and the BESS (e.g., state of charge (SOC), real-time reserve).

Abstract—With increasing penetrations of wind generation on electric grids, wind power plants (WPPs) are encouraged to provide frequency ancillary services (FAS); however, it is a challenge to ensure that variable wind generation can reliably provide these ancillary services. This paper proposes using a battery energy storage system (BESS) to ensure the WPPs' commitment to FAS. This method also focuses on reducing the BESS's size and extending its lifetime. In this paper, a state-machine-based coordinated control strategy is developed to utilize a BESS to support the obliged FAS of a WPP (including both primary and secondary frequency control). This method takes into account the operational constraints of the WPP (e.g., real-time reserve) and the BESS (e.g., state of charge (SOC), real-time reserve).

R_{SG}

f_{sys}
WTGs
WPP

P_{WPP_Dis}

P_{WPP_AGC}
 P_{WPP_PFC}
 P_{WPP_Order}

Dynamic reserve of the synchronous generators.
Power system frequency.
Wind turbine generators.
Wind power plant.
Power command from economic dispatch (every 5 minutes).
AGC signal (every 4 seconds).
Power used for PFC support.
Power command of the WPP.
State of charge (SOC) of BESS at generator i .

Lower and upper SOC limit of BESS.
Energy stored in BESS at time t (MWh).
Rated energy capacity of BESS (MWh).

Capacity Optimization of Renewable Energy Sources and Battery Storage in an Autonomous Telecommunication Facility

Tomislav Dragičević, *Member, IEEE*, Hrvoje Pandžić, *Member, IEEE*, Davor Škrlec, *Member, IEEE*, Igor Kuzle, *Senior Member, IEEE*, Josep M. Guerrero, *Senior Member, IEEE*, and Daniel S. Kirschen, *Fellow, IEEE*

Abstract—This paper describes a robust optimization approach to minimize the total cost of supplying a remote telecommunication station exclusively by renewable energy sources (RES). Due to the intermittent nature of RES, such as photovoltaic (PV) panels and small wind turbines, they are normally supported by a central energy storage system (ESS), consisting of a battery and a fuel cell. The optimization is carried out as a robust mixed-integer linear program (RMILP), and results in different optimal solutions, depending on budgets of uncertainty, each of which yields different RES and storage capacities. These solutions are then tested against a set of possible outcomes, thus simulating the future operation of the system. Since battery cycling is inevitable in this application, an algorithm that counts the number of cycles and associated depths of

K_w	Wind turbine specific cost (€/kW).
$PV^{\max}(t)$	Normalized maximum PV output (kW/kW).
S^{\min}	Minimum allowed state-of-charge (SoC) (%).
$W^{\max}(t)$	Normalized maximum wind turbine output (kW/kW).
η_{ch}	Charging efficiency of the battery.
η_{dis}	Discharging efficiency of the battery.
<i>Variables</i>	
c_{bat}	Total battery storage capacity (kWh).
c_{fc}	Fuel cell installed capacity (kW).

Batteries in Microgrids

227

IEEE TRANSACTIONS ON SMART GRID, VOL. 7, NO. 1, JANUARY 2016

Bidding Strategy for Microgrid in Day-Ahead Market Based on Hybrid Stochastic/Robust Optimization

Guodong Liu, *Student Member, IEEE*, Yan Xu, *Member, IEEE*, and Kevin Tomsovic, *Fellow, IEEE*

Abstract—This paper proposes an optimal bidding strategy in the day-ahead market of a microgrid consisting of intermittent distributed generation (DG), storage, dispatchable DG, and price responsive loads. The microgrid coordinates the energy consumption or production of its components, and trades electricity in both day-ahead and real-time markets to minimize its operating cost as a single entity. The bidding problem is challenging due to a variety of uncertainties, including power output of intermittent DG, load variation, and day-ahead and real-time market prices. A hybrid stochastic/robust optimization model is proposed to minimize the expected net cost, i.e., expected total cost of operation minus total benefit of demand. This formulation can be solved by mixed-integer linear programming. The uncertain output of

 j
 s
 t
 p
 w
 m

Index of responsive demands, running from 1 to N_D .

Index of battery storage devices, running from 1 to N_S .

Index of time periods, running from 1 to N_T .

Index of stage 1 scenarios of day-ahead market prices, running from 1 to N_P .

Index of stage 2 scenarios of wind and photovoltaic (PV), running from 1 to N_W .

Index of energy blocks offered by generators (demand), running from 1 to N_I (N_J).

Capacity (kW).

Optimal Operation and Services Scheduling for an Electric Vehicle Battery Swapping Station

Mushfiqu R. Sarker, *Student Member, IEEE*, Hrvoje Pandžić, *Member, IEEE*, and Miguel A. Ortega-Vazquez, *Member, IEEE*

Abstract—For a successful rollout of electric vehicles (EVs), it is required to establish an adequate charging infrastructure. The adequate access to such infrastructure would help to mitigate concerns associated with limited EV range and long charging times. Battery swapping stations are poised as effective means of eliminating the long waiting times associated with charging the EV batteries. These stations are mediators between the power system and their customers. In order to successfully deploy this type of stations, a business and operating model is required, that will allow it to generate profits while offering a fast and reliable alternative to charging batteries. This paper proposes an optimization framework for the operating model of battery swapping stations. The proposed model considers the day-ahead scheduling process. Battery demand uncertainty is modeled using inventory robust optimization, while multi-band robust optimization is employed to

Continuous Variables:

$bat_{i,t}^{chg}$	Charging power of battery i at period t (kW).
$bat_{i,t}^{dsg}$	Discharging power of battery i at period t (kW).
$C_{i,t}^{deg}$	Degradation cost for battery i at period t (\$).
em_t^{buy}	Energy purchased in the wholesale market at period t (kWh).
em_t^{sell}	Energy sold in the wholesale market at period t (kWh).
$L_{i,t,d}$	Energy shortage with respect to the discount curve for battery i in each discount segment d at period

IEEE TRANSACTIONS ON POWER SYSTEMS, VOL. 30, NO. 5, SEPTEMBER 2015

Optimal Bidding Strategy of a Plug-In Electric Vehicle Aggregator in Day-Ahead Electricity Markets Under Uncertainty

Marina González Vayá, *Student Member, IEEE*, and Göran Andersson, *Fellow, IEEE*

Abstract—With a large-scale introduction of plug-in electric vehicles (PEVs), a new entity, the PEV fleet aggregator, is expected to be responsible for managing the charging of, and for purchasing electricity for, the vehicles. We approach the problem of an aggregator bidding into the day-ahead electricity market with the objective of minimizing charging costs while satisfying the PEVs' flexible demand. The aggregator places demand bids only (no vehicle-to-grid is considered). The aggregator is assumed to potentially influence market prices, in contrast to what is commonly found in the literature. Specifically, the bidding strategy of the aggregator is formulated as a bilevel problem, which is implemented as a mixed-integer linear program. The upper level problem represents the charging cost minimization of the aggregator, whereas

- $P_{c,\max}^t$ Upper bound of aggregated charging power at time t .
- $P_{c,\min}^t$ Lower bound of aggregated charging power at time t .
- ϵ Constraint violation parameter.
- β Confidence parameter.
- n_m Number of stochastic constraints.
- $b_{s_m}^t$ Price of supply bid s_m at time t .
- $b_{d_k}^t$ Price of demand bid d_k at time t .
- L Very large number.
- u_i^t Indicates if vehicle v_i is connected at time t (0 if not connected with respect to the discount curve for battery i in each discount segment d at period

A Game Theoretic Approach to Risk-Based Optimal Bidding Strategies for Electric Vehicle Aggregators in Electricity Markets With Variable Wind Energy Resources

Hongyu Wu, *Member, IEEE*, Mohammad Shahidehpour, *Fellow, IEEE*,
Ahmed Alabdulwahab, *Senior Member, IEEE*, and Abdullah Abusorrah, *Senior Member, IEEE*

Abstract—This paper proposes a stochastic optimization model for optimal bidding strategies of electric vehicle (EV) aggregators in day-ahead energy and ancillary services markets with variable wind energy. The forecast errors of EV fleet characteristics, hourly loads, and wind energy as well as random outages of generating units and transmission lines are considered as potential uncertainties, which are represented by scenarios in the Monte Carlo Simulation (MCS). The conditional value at risk (CVaR) index is utilized for measuring EV aggregators' risks caused by the uncertainties. The EV aggregator's optimal bidding strategy is formulated as a mathematical programming with equilibrium constraints (MPEC), in which the upper level problem is the aggregators' CVaR maximization while the lower level problem is a mixed-integer linear programming that represents the charging cost minimization.

- i Index for thermal generating units.
- c Index for EV fleets.
- d Index for buses.
- k Index for wind generators.
- m Index for blocks of thermal unit dispatch.
- s Index for base case $s = 0$ and scenarios.

Sets and Signs

- Θ_n Set of EV fleets controlled by aggregator n .
- TP_n Set of types of EV aggregator.
- Q, NQ Set of quick-start/non-quick-start thermal generating

t.
t.

if not
curve
period

Batteries in Electric Vehicles

374

221

IEEE TRANSACTIONS ON POWER SYSTEMS, VOL. 29, NO. 1, JANUARY 2014

61

Electric Vehicle Battery Charging/Swap Stations in Distribution Systems: Comparison Study and Optimal Planning

Yu Zheng, *Student Member, IEEE*, Zhao Yang Dong, *Senior Member, IEEE*, Yan Xu, *Member, IEEE*, Ke Meng, *Member, IEEE*, Jun Hua Zhao, *Member, IEEE*, and Jing Qiu, *Student Member, IEEE*

Abstract—Electric vehicle (EV) is a promising technology for reducing environmental impacts of road transport. In this paper, a framework for optimal design of battery charging/swap stations in distribution systems based on life cycle cost (LCC) is presented. The battery charging/swap station models are developed to compare the impacts of rapid-charging stations and battery swap stations. Meanwhile, in order to meet the requirements of increased power provided during the charging period, the distribution network should be reinforced. In order to control this reinforcement cost, stations should be placed at appropriate places and be scaled correctly. For optimal cost-benefit analysis and safety operation, the LCC criterion is used to assess the project and a modified dif-

C_k	One-time investment of charging station k (\$).
C_l	Investment of reinforce equipment l (\$)
C_{no}	Operation cost of the distribution networks.
C_{so}	Operation cost of the charging station.
CI	Investment costs.
CO	Operation costs.
CM	Maintenance costs.
	Set of EV aggregator n .
	Set of quick-start/non-quick-start thermal generating

curve
period

What do all of These Models Have in Common?

- They use the same battery model :

$$soc_h(t) = soc_h(t-1) + q_h^{ch}(t) \cdot \eta^{ch} - \frac{q_h^{dis}(t)}{\eta^{dis}}$$

$$0 \leq soc_h(t) \leq soc_h^{max}$$

$$q_h^{dis}(t) \leq dis_h^{max}$$

$$q_h^{ch}(t) \leq ch_h^{max}$$

Rechargeable Batteries

- Common technologies:
 - Lead acid
 - Nickel based
 - Nickel-cadmium (NiCd)
 - Nickel-metal-hydride (NiMH)
 - Lithium-ion (li-ion)
- Generally speaking – all rechargeable battery technologies have similar characteristics
- Today's practical demonstration:
 - Li-ion cell
 - Lead acid battery pack

Rechargeable Batteries

- ❑ Main characteristics: voltage and capacity
- ❑ Capacity – ampere-hours (Ah) or watt-hours (Wh)
 - E.g. battery rated at 10 Ah delivers:
 - ❑ Current of 10 A for 1 hour
 - ❑ Current of 5 A for 2 hours, etc.
 - Capacity degrades with time and usage
- ❑ C-rate = battery charging/discharging speed
 - 1C corresponds to Ah rating, e.g.:
 - ❑ 1C for a 10 Ah battery = 10 A
 - ❑ 2C for a 10 Ah battery = 20 A
 - ❑ 0.5C for a 10 Ah battery = 5 A

Rechargeable Batteries

- Battery price
 - Usually expressed per unit energy
 - \$/kWh
 - Price of a new li-ion battery is cca. 500-800 \$/kWh
- Specific energy
 - Defines battery capacity per unit mass
 - Wh/kg
- Energy density
 - Defines battery capacity per unit volume
 - Wh/l
- Specific power
 - Maximum available power per unit mass
 - W/kg
- Power density
 - Maximum available power per unit volume
 - W/l



Series/Parallel Configurations

- Series connection
 - Increases voltage
- Parallel connection
 - Increases maximum current
 - Increases Ah-capacity
- Battery energy (Wh-capacity)
 - Does not change with series/parallel configuration
 - Depends on the total number of connected cells

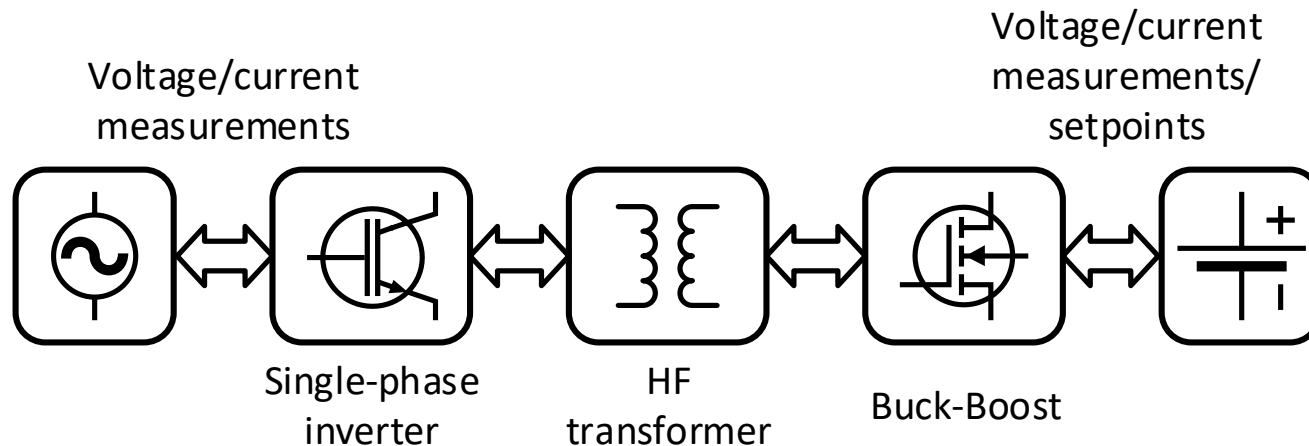


Custom-Made Converter

- ❑ Custom made bidirectional AC/DC converter for battery charging/discharging
- ❑ Specifications:
 - Nominal output power: 1 kW
 - Output voltage: 0 – 20 VDC
 - Output current: -50 to 50 ADC
 - Input: 50 Hz, 230 VAC
 - Input/output voltage/current measurements
 - ❑ Analog signals 0 – 10 VDC
 - ❑ Digital signals via isolated USB or RS-485
 - Remote battery voltage sensing (increased accuracy)

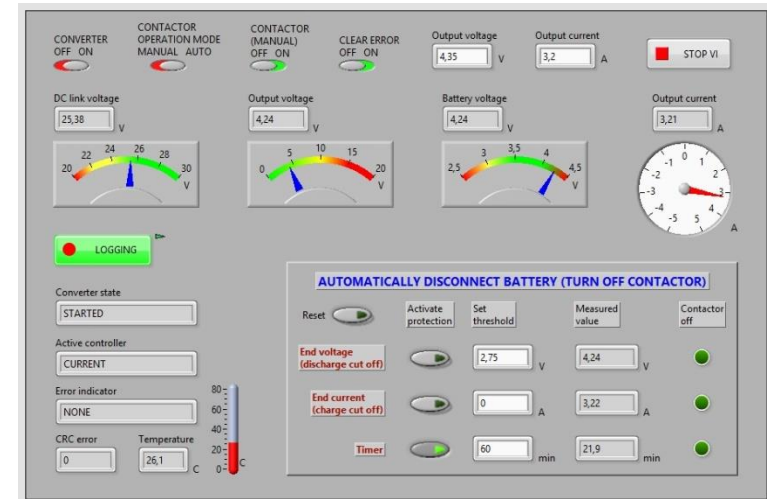
Custom-Made Converter

- Three-stage topology
 - Bidirectional grid inverter
 - Resonant HF transformer
 - Output bidirectional interleaved buck-boost converter

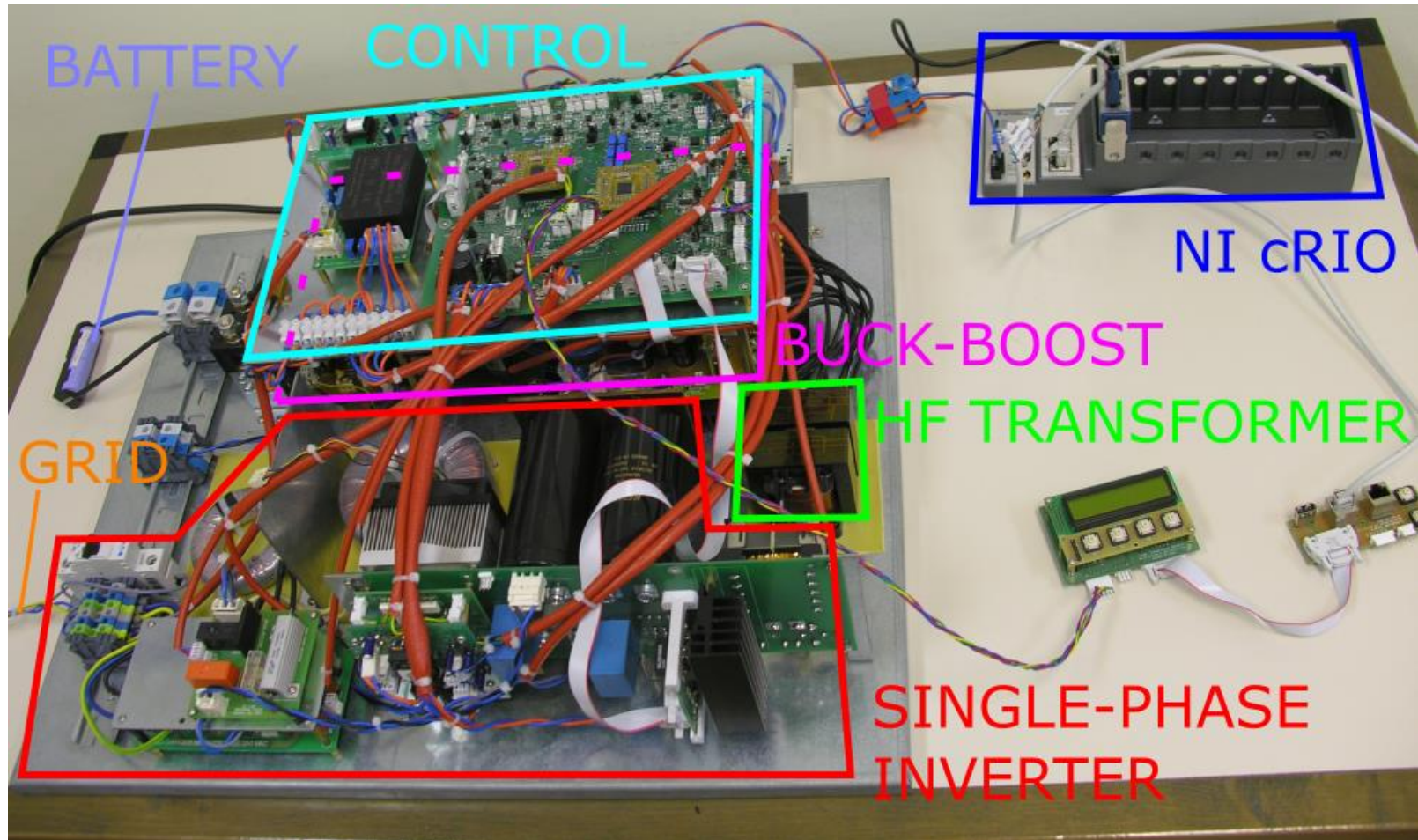


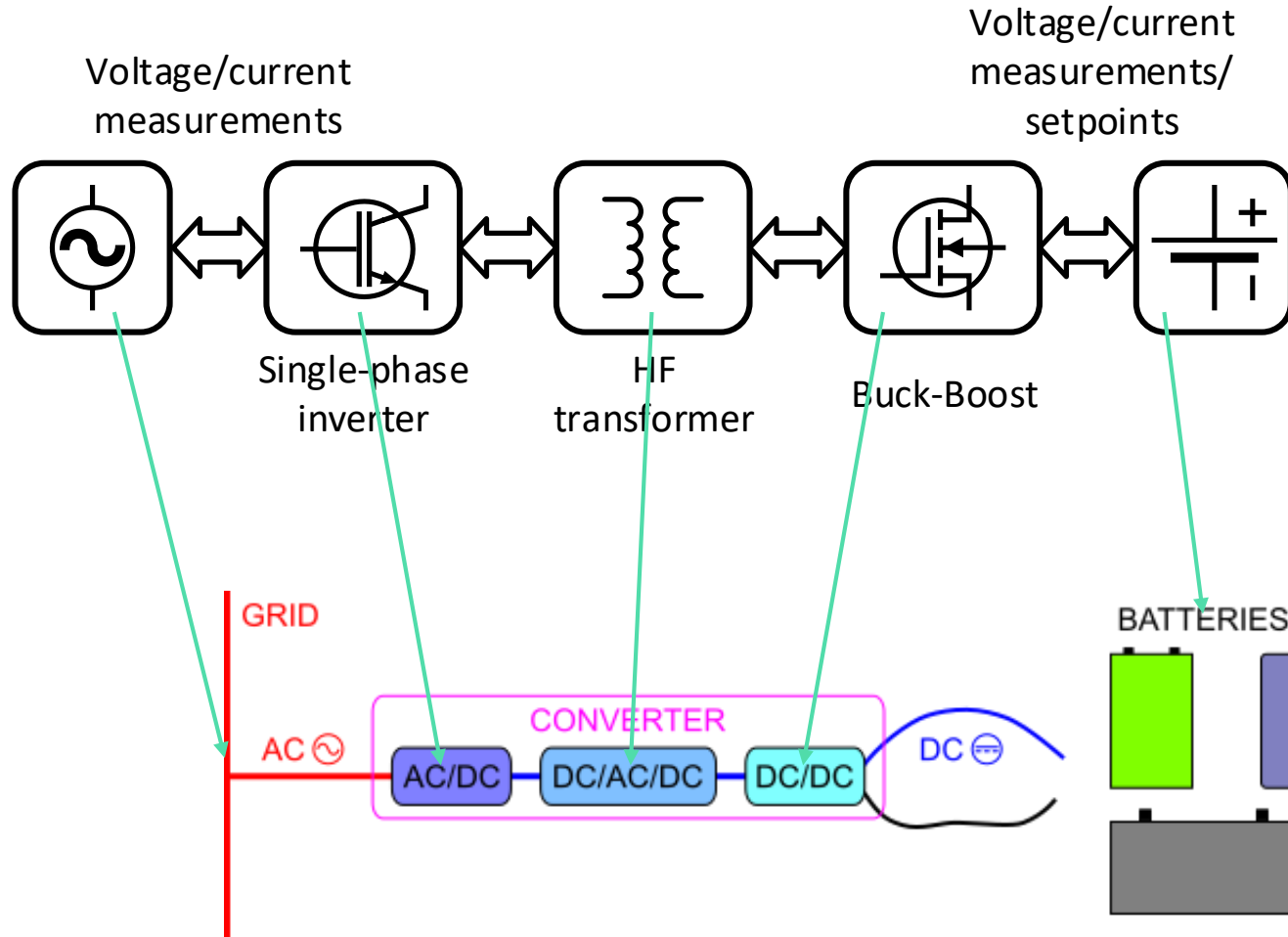
Custom-Made Converter

- Communication and control – NI LabVIEW
- Converter is connected to host PC
 - Communication – NI cRIO via Ethernet
 - SCADA – NI LabVIEW



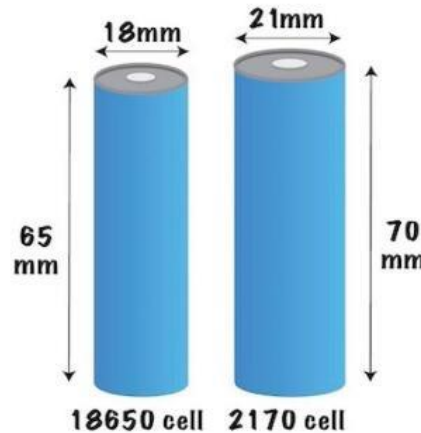
Custom-Made Converter





Lithium-ion batteries

- The most widespread battery technology is lithium-ion (li-ion)
- Li-ion cell types
 - Cylindrical
 - 18650
 - 21700
 - Prismatic
 - Pouch
 - Commonly Li-polymer



Experimental Research

□ 18650 li-ion cells

- Tesla model S
- Laptop computers
- Power tools, etc.



□ Samsung ICR18650-32A

- Chemistry: Lithium Cobalt Oxide (LiCoO_2) – LCO or ICR
- Nominal voltage: 3.75 V
- Nominal capacity: 3.2 Ah
- Minimum capacity: 3.1 Ah





Datasheet – ICR18650-32A

2. Description and Model

2.1 Description Cell (lithium-ion rechargeable cell)

2.2 Model ICR18650-32A

3. Nominal Specifications

Item	Specification
3.1 Nominal Capacity	3200 mAh (0.2 C, 2.75 V discharge)
3.2 Minimum Capacity	3100 mAh (0.2 C, 2.75 V discharge)
3.3 Charging Voltage	4.35 ±0.03 V
3.4 Nominal Voltage	3.75
3.5 Charging Method	CC-CV (constant voltage with limited current)
3.6 Charging Current	Standard charge: 1600 mA Rapid charge : 3200 mA
3.7 Charging Time	Standard charge : 3 hours Rapid charge : 2.5 hours
3.8 Max. Charge Current	3200mA(ambient temperature 25 ℃)
3.9 Max. Discharge Current	6400mA(ambient temperature 25 ℃)
3.10 Discharge Cut-off Voltage	2.75 V
3.11 Cell Weight	50.0 g max
3.12 Cell Dimension	Height : 65.00 mm max Diameter : 18.40 mm max
3.13 Operating Temperature	Charge : 0 to 45 ℃ Discharge: -20 to 60 ℃
3.14 Storage Temperature	1 year : -20~25 ℃(1*) 3 months : -20~45 ℃(1*) 1 month : -20~50 ℃(1*)

Charging Characteristic

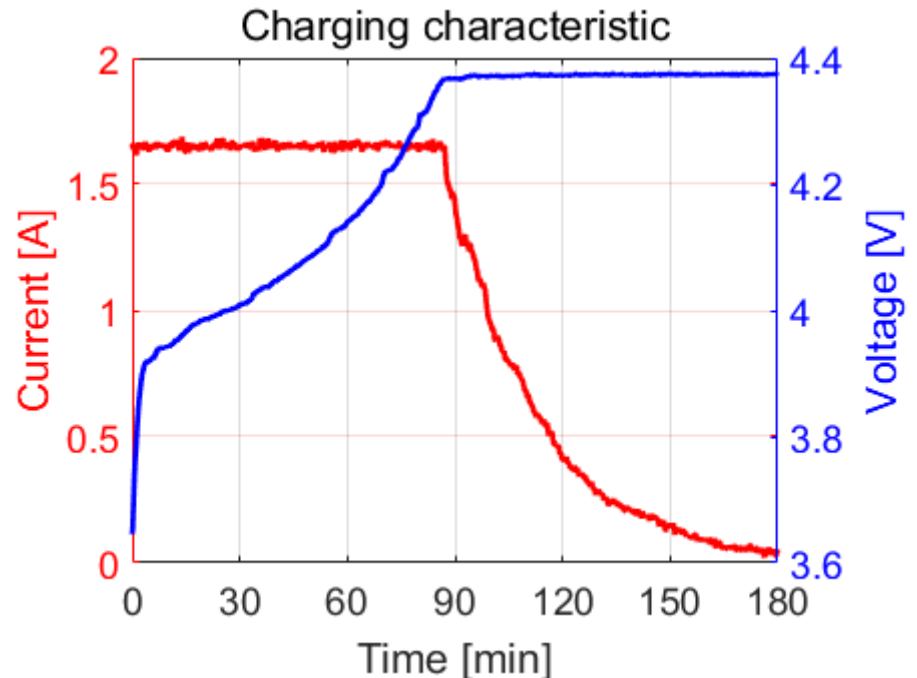
- ❑ Constant-current/constant-voltage (CC/CV) charging
 1. Current is constant while voltage rises to a predefined threshold
 2. Voltage is constant while current gradually decreases
 3. Full charge is reached after the current drops to some small value (typically 3-5% of the Ah rating)
- ❑ Adjustable parameters:
 - Constant charging current
 - Voltage threshold
 - Cut-off current

Charging Characteristic

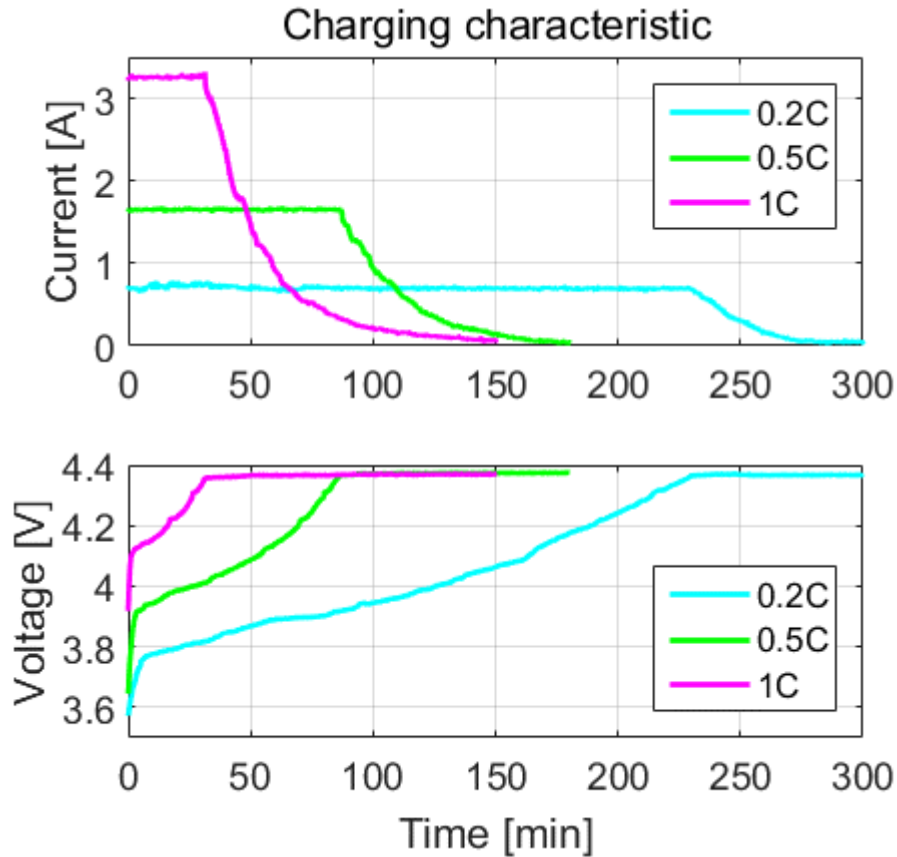
□ Charging conditions:

- Constant current: 1.6 A (0.5C)
- Voltage threshold: 4.35 V
- Duration: 180 min

Experimentally
obtained



Charging Characteristic



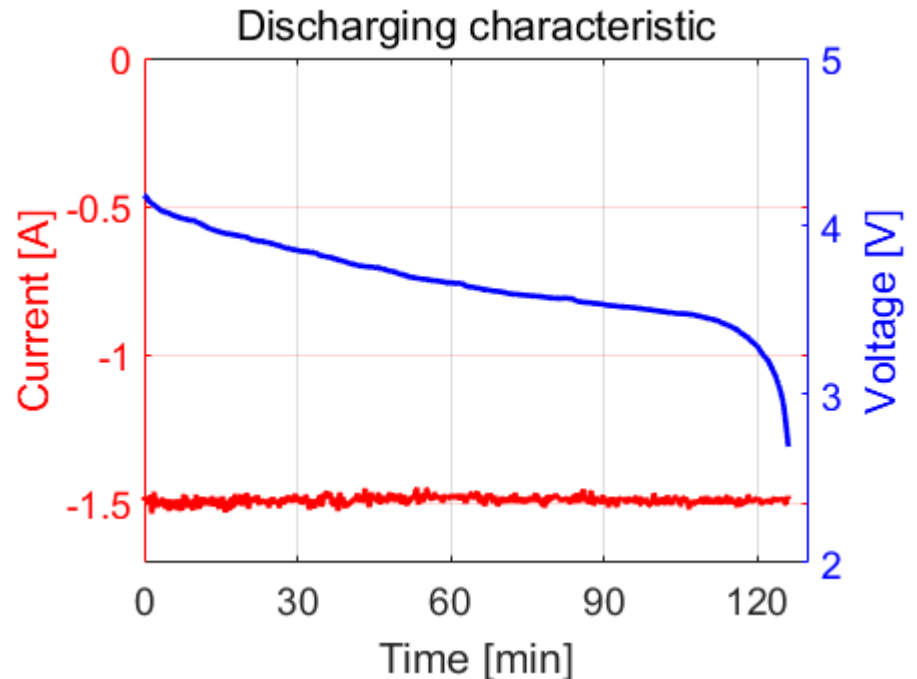
Experimentally
obtained

Discharging Characteristic

- Current profile depends on the application
 - Varying current – various practical applications
 - Constant current (CC) – laboratory experiments
- Full discharge is reached after voltage drops to some predefined cut-off value
- Unlike charging duration, discharge durations are approximately consistent with the C-rate
 - 0.5C – cca. 2 hours
 - 1C – cca. 1 hour
 - 2C – cca. 30 minutes

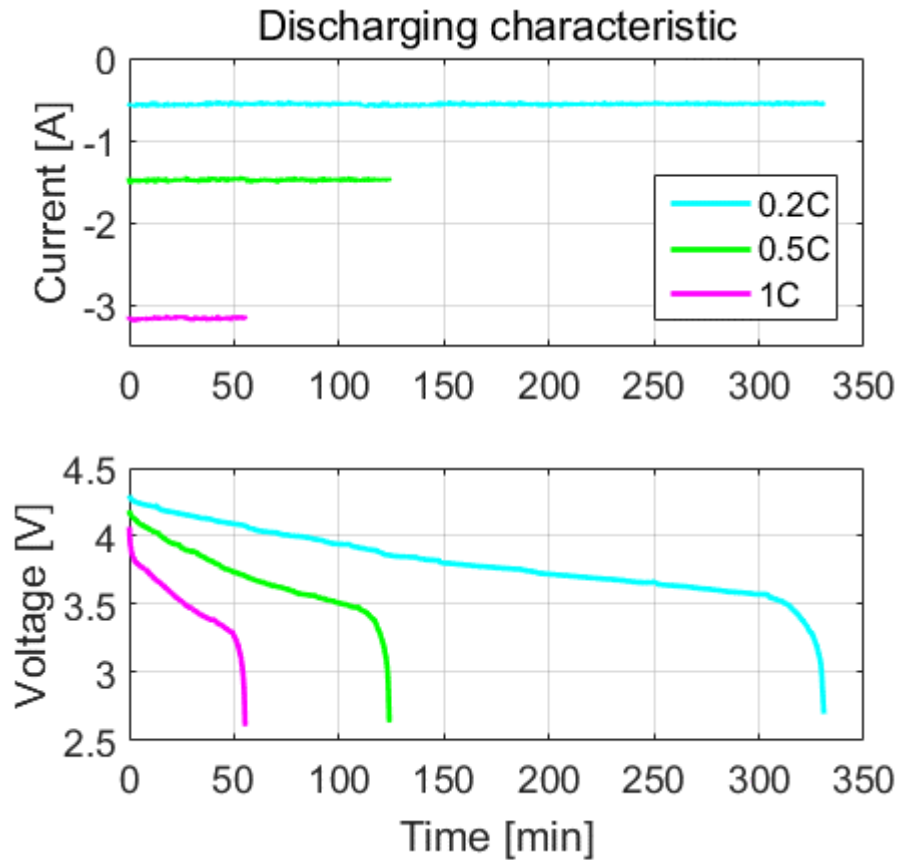
Discharging Characteristic

- Discharging conditions:
 - Constant current: 1.6 A (0.5C)
 - Cut-off voltage: 2.75 V



Experimentally
obtained

Discharging Characteristic



Experimentally
obtained

State-of-Charge (SoC)

- SoC measured against charging duration
- Series of partial charges applied (10-min steps) followed by immediate controlled full discharge

■ Cut-off voltage: 2.75 V

- $SoC (Ah) =$

$$\sum_{k=1}^N \frac{I_{dis}(\tau_{k-1}) + I_{dis}(\tau_k)}{2} \Delta \tau_k$$

- Charging:

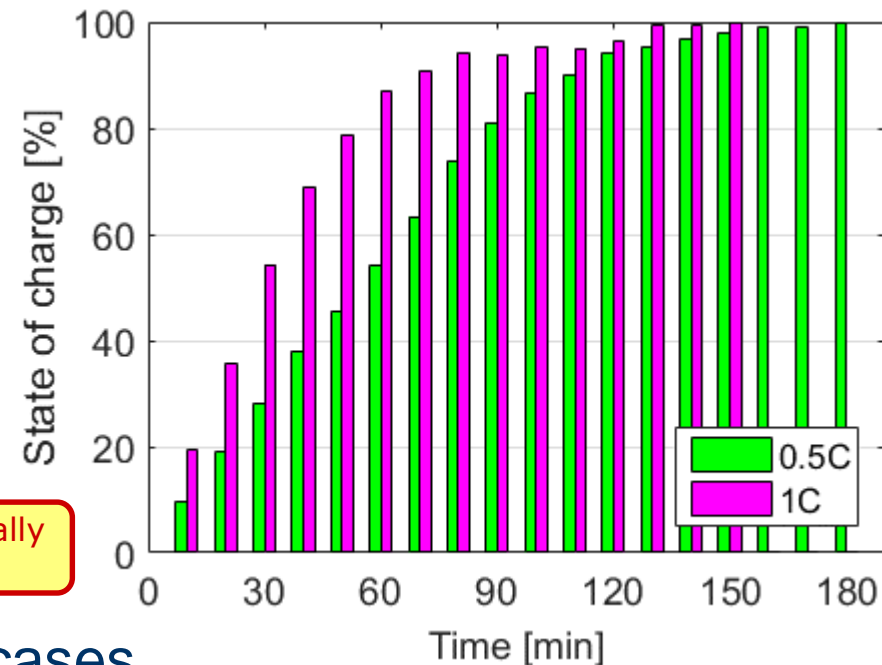
■ $I_{ch} = 1.6 A (0.5C)$

■ $I_{ch} = 3.2 A (1C)$

- Discharging:

■ $I_{dis} = 1.6 A (0.5C)$ – both cases

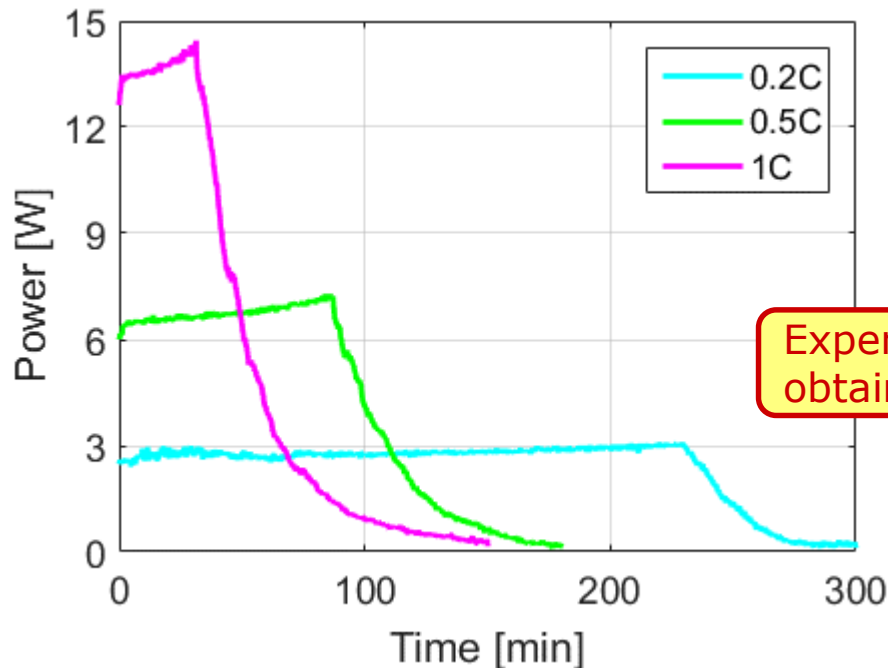
Experimentally
obtained



Charging Power and Energy

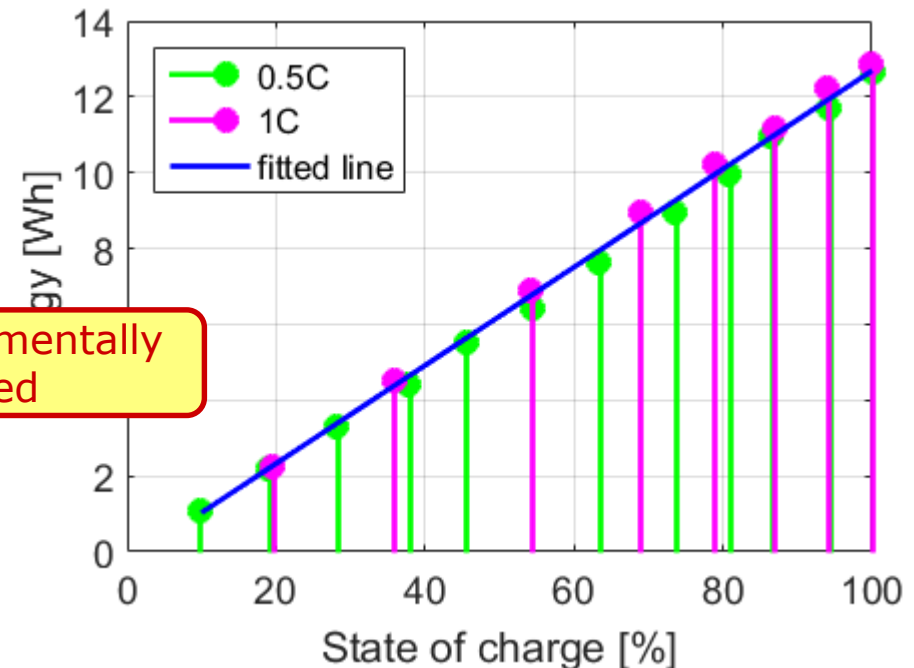
- Electrical power characteristic during full charge (0%-100% SoC)

- $P = U \cdot I$; [W=V·A]



- Electrical energy:
 $E = \int_0^t P(\tau) d\tau$; [J=W·h]

- Full charge energy:
12.6 Wh (0.5C), 12.9 Wh (1C)

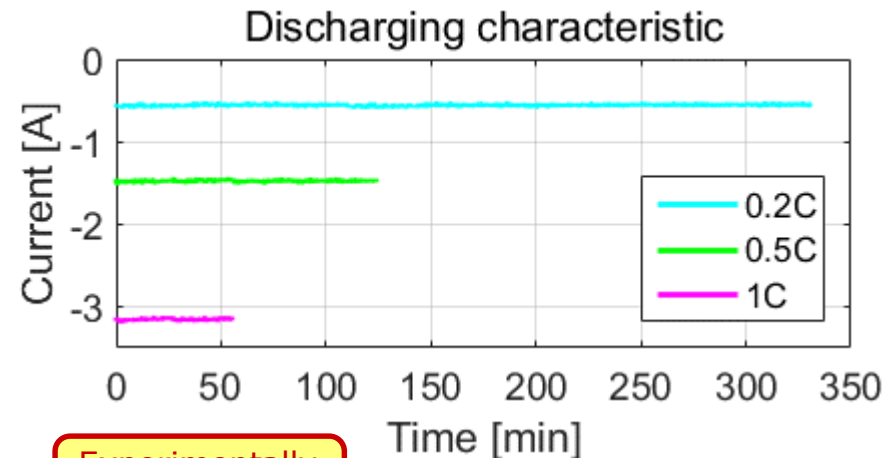


Capacity

- Maximal number of Ampere-hours (Ah), or Watt-hours (Wh), that can be drawn from a battery on a single discharge
- Fully charged battery → discharge to cut-off voltage

$$\square C (Ah) = \int_0^T I_{dis}(\tau) d\tau$$

$$\square C_E (Wh) = \int_0^T P_{dis}(\tau) d\tau$$



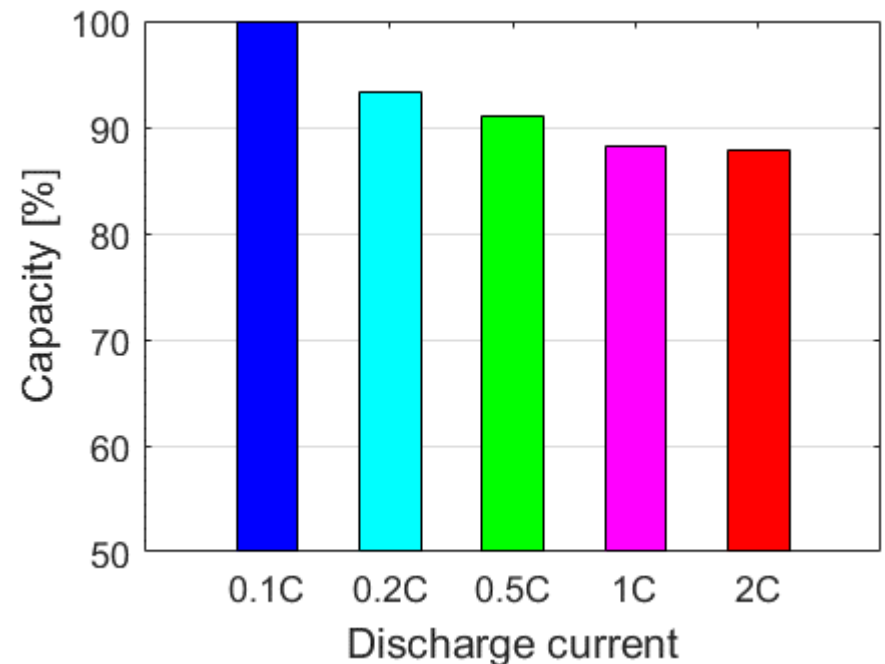
Experimentally
obtained

Rate Capacity Effect

- Higher discharge current = lower capacity
- Also known as "Peukert's law"
 - Applied mostly to lead-acid batteries

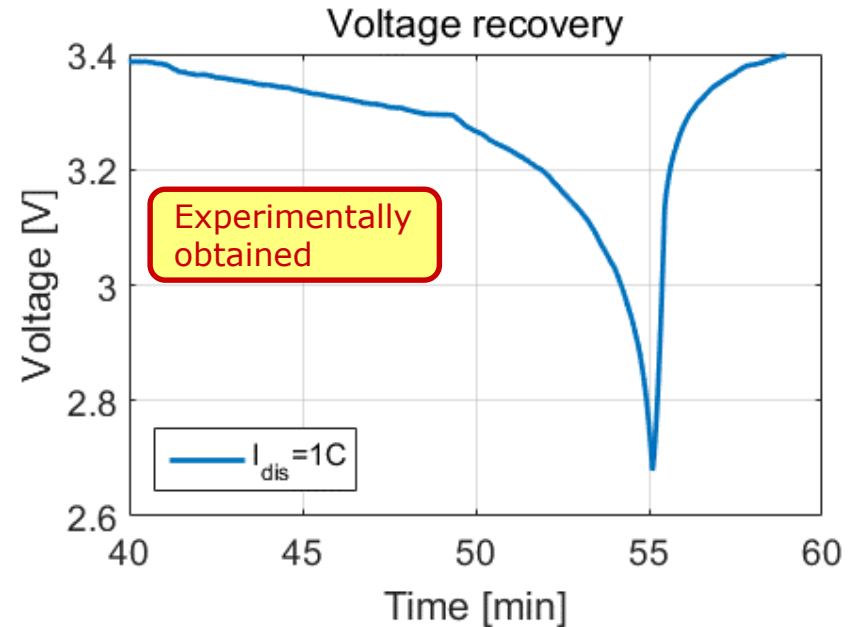
Experimentally
obtained

100% capacity = 3.3 Ah



Capacity Recovery Effect

- End of discharge \leftrightarrow predefined cut-off voltage
- Waiting period after end of discharge \rightarrow voltage recovers \rightarrow battery can be discharged further



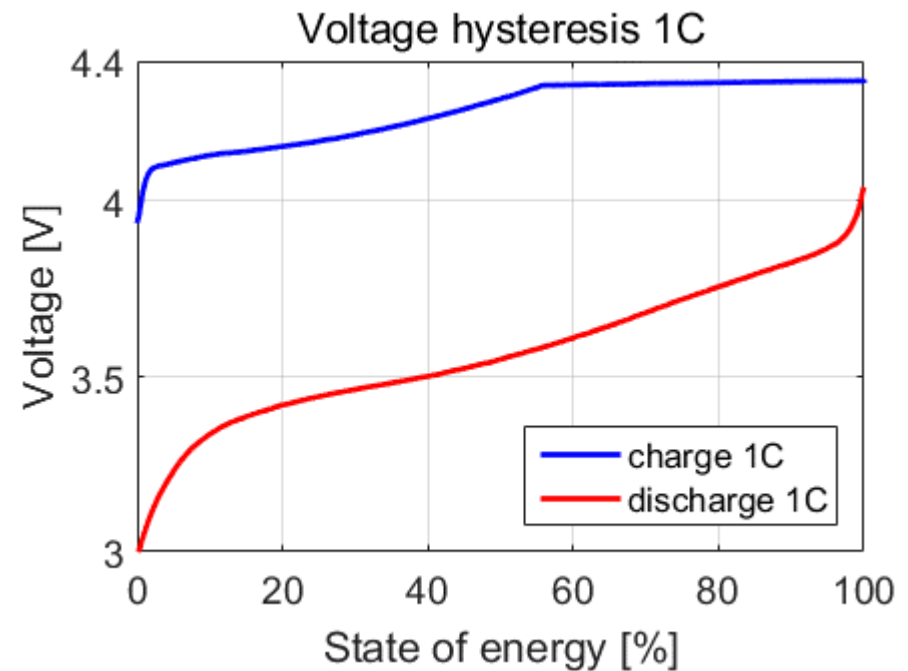
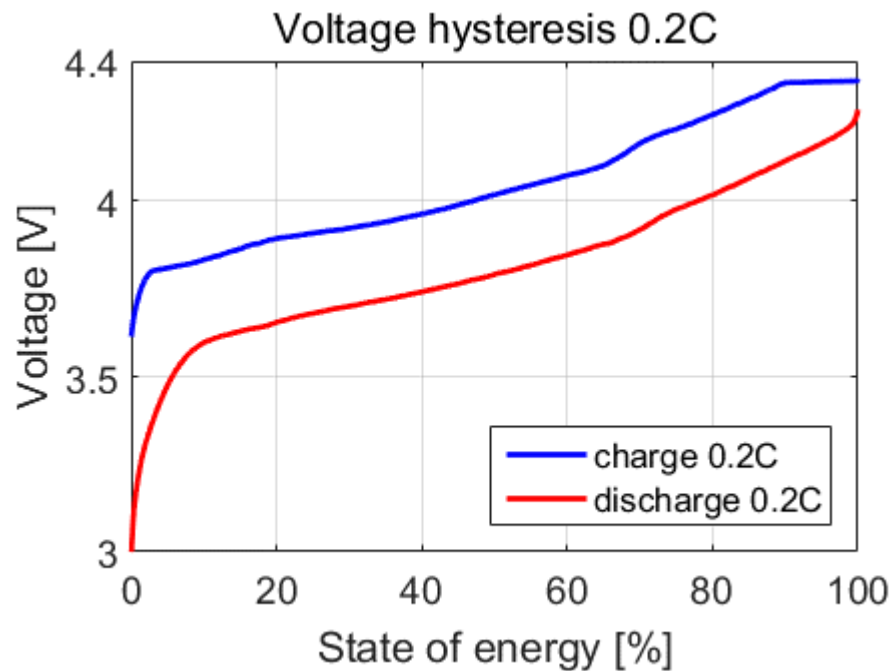
- This effect is more expressed for higher discharge currents
 - The higher the current during first discharge, the more Ah can be extracted on a second discharge (after the waiting period)
- This effect becomes insignificant for relatively low discharge currents – 0.1C and lower

Internal Resistance

- ❑ Every battery has internal resistance from:
 - Electrodes
 - Electrolyte
 - Connections, wiring etc.
- ❑ Causes voltage drop when charge/discharge current is applied
 - Ohm's law: $U = I \cdot R$
- ❑ Open circuit voltage (OCV) \leftrightarrow no current flow
- ❑ Closed circuit voltage (CCV) \leftrightarrow current flow
 - Charging – raises CCV
 - Discharging – lowers CCV
 - "Rubber band effect"

Internal Resistance

Voltage drop due to internal resistance



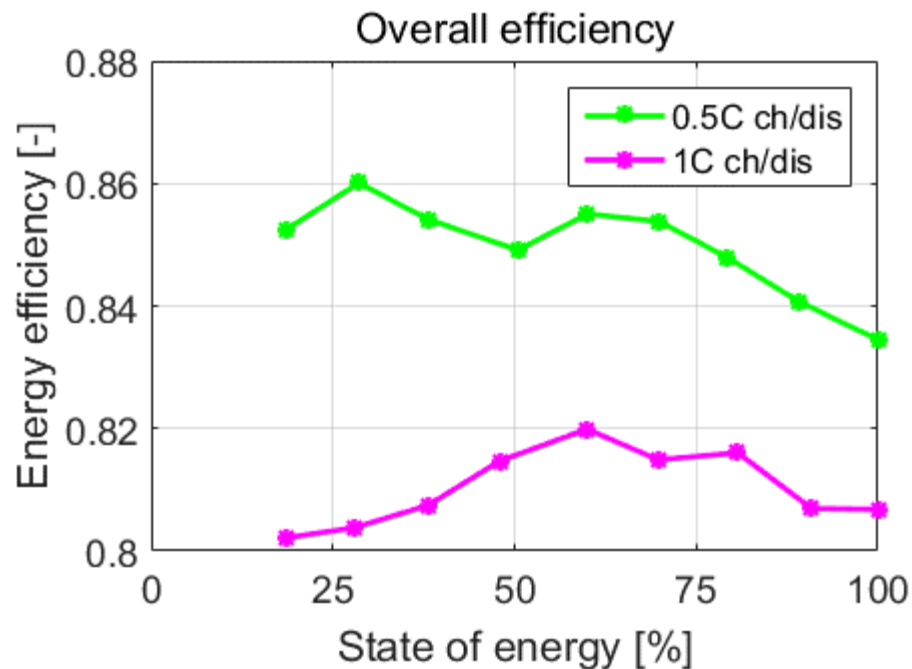
Experimentally
obtained

Battery Efficiency

- Cause of energy losses – internal resistance
→ heat dissipation
- Types of efficiencies (1):
 - Coulombic
 - Voltaic
 - Energy (includes both coulombic and voltaic)
- Types of efficiencies (2):
 - Charging
 - Discharging
 - Overall (charging + discharging)

Battery Efficiency

Efficiency is predominantly dependent on the charging/discharging current



Experimentally
obtained

Bact to This Formulation...

$$soc_h(t) = soc_h(t-1) + q_h^{\text{ch}}(t) \cdot \eta^{\text{ch}} - \frac{q_h^{\text{dis}}(t)}{\eta^{\text{dis}}}$$

$$0 \leq soc_h(t) \leq soc_h^{\text{max}}$$

$$q_h^{\text{dis}}(t) \leq dis_h^{\text{max}}$$

$$q_h^{\text{ch}}(t) \leq ch_h^{\text{max}}$$

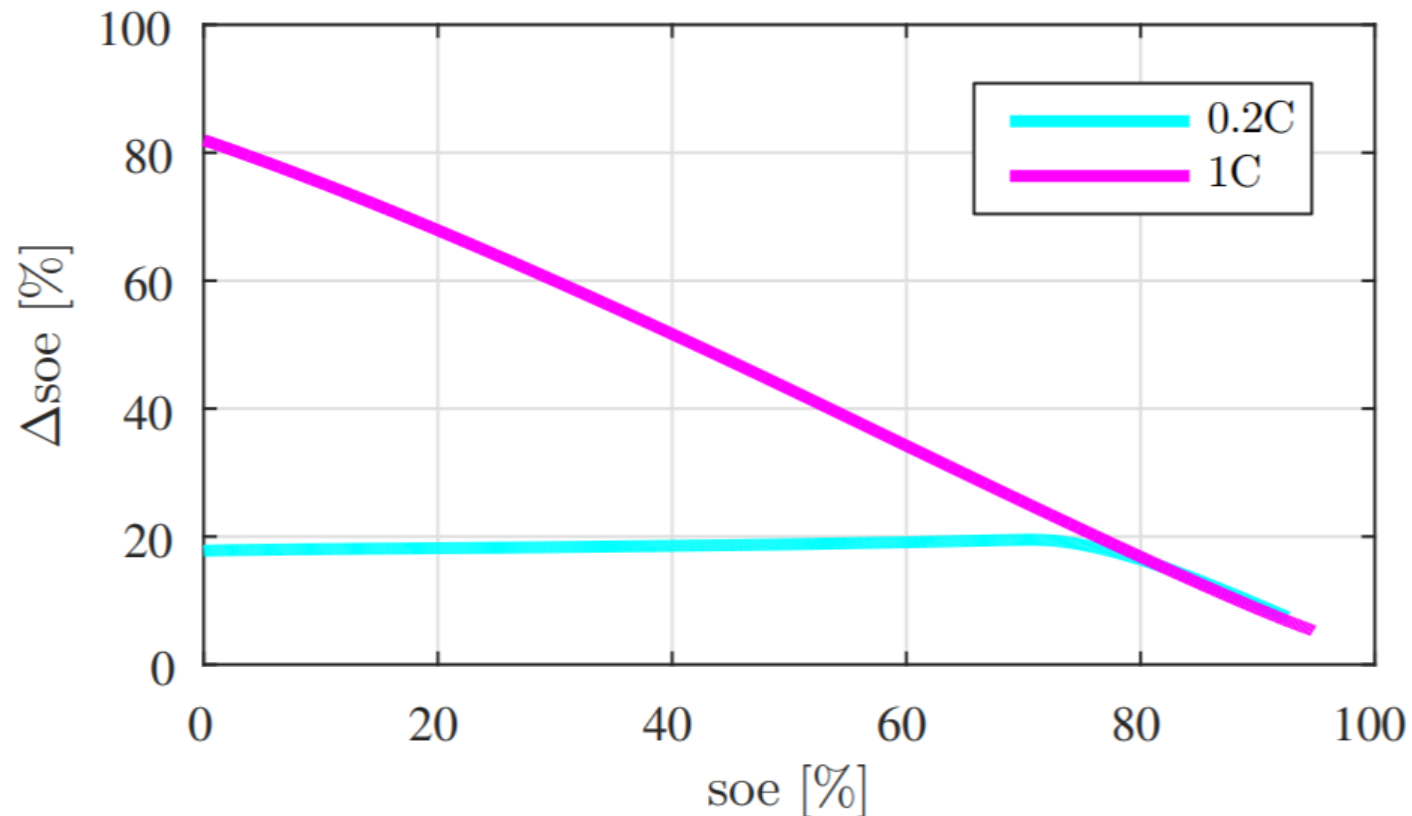
Improvement

$$ch_t \leq P^{\text{ch}} \cdot \frac{SOE^{\text{max}} - soe_t}{SOE^{\text{max}} - SOE^{\text{cc,cv}}}$$

S. I. Vagropoulos and A. G. Bakirtzis, "Optimal Bidding Strategy for Electric Vehicle Aggregators in Electricity Markets," in *IEEE Transactions on Power Systems*, vol. 28, no. 4, pp. 4031-4041, Nov. 2013.

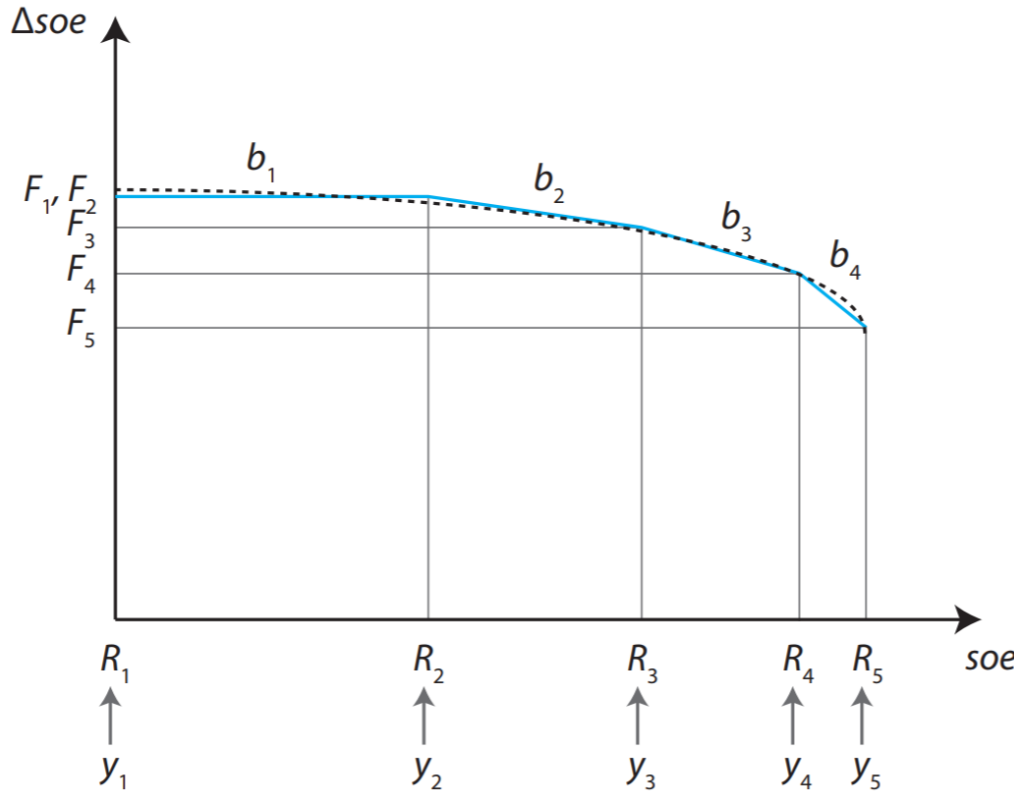
Let's Talk Energy

- Battery hour-ahead energy charging ability



Approximation

□ Approximation of the Δsoe — soe function using SOS2



$$soe_t = \sum_{i=1}^I R_i \cdot y_{t,i}, \quad \forall t \in T$$

$$0 \leq y_{t,i} \leq 1, \quad \forall t \in T, i \in I$$

$$\sum_{i=1}^I y_{t,i} = 1, \quad \forall t \in T$$

$$\begin{bmatrix} y_{t,1} \\ y_{t,2} \\ \vdots \\ y_{t,I} \end{bmatrix} \leq [\mathbf{H}] \begin{bmatrix} b_{t,1} \\ b_{t,2} \\ \vdots \\ b_{t,I-1} \end{bmatrix}$$

$$\sum_{i=1}^{I-1} b_{t,i} = 1, \quad \forall t \in T$$

$$\Delta soe_t = \sum_{i=1}^I F_i \cdot y_{t,i}, \quad \forall t \in T$$

$$ch_t \leq \Delta soe_t / \Delta t, \quad \forall t \in T$$

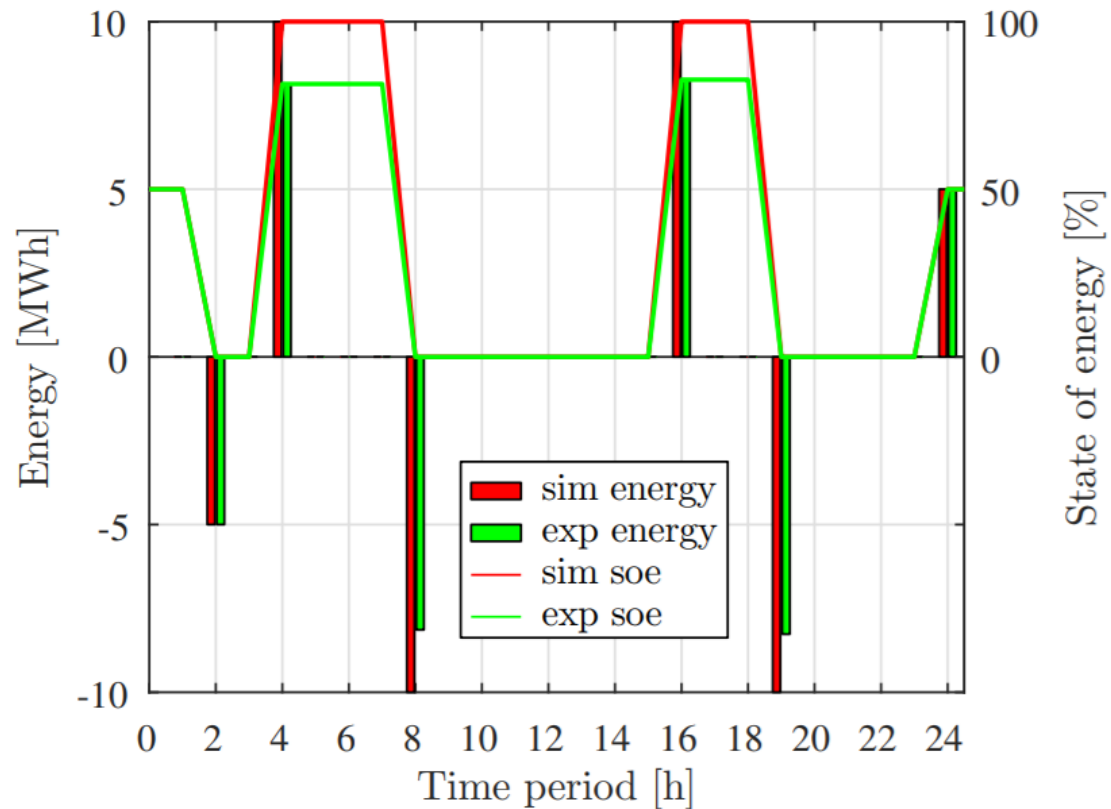
Case Study

- ❑ 10 MWh battery scaled to laboratory capacity of 10 Wh
- ❑ Acting in the EPEX day-ahead market, prices on January 15, 2018.
- ❑ The obtained (dis)charging schedules of each of the models, i.e. the baseline mode, the linear CC-CV model and the proposed energy charging model, are then verified for feasibility in a laboratory experiment

Case Study

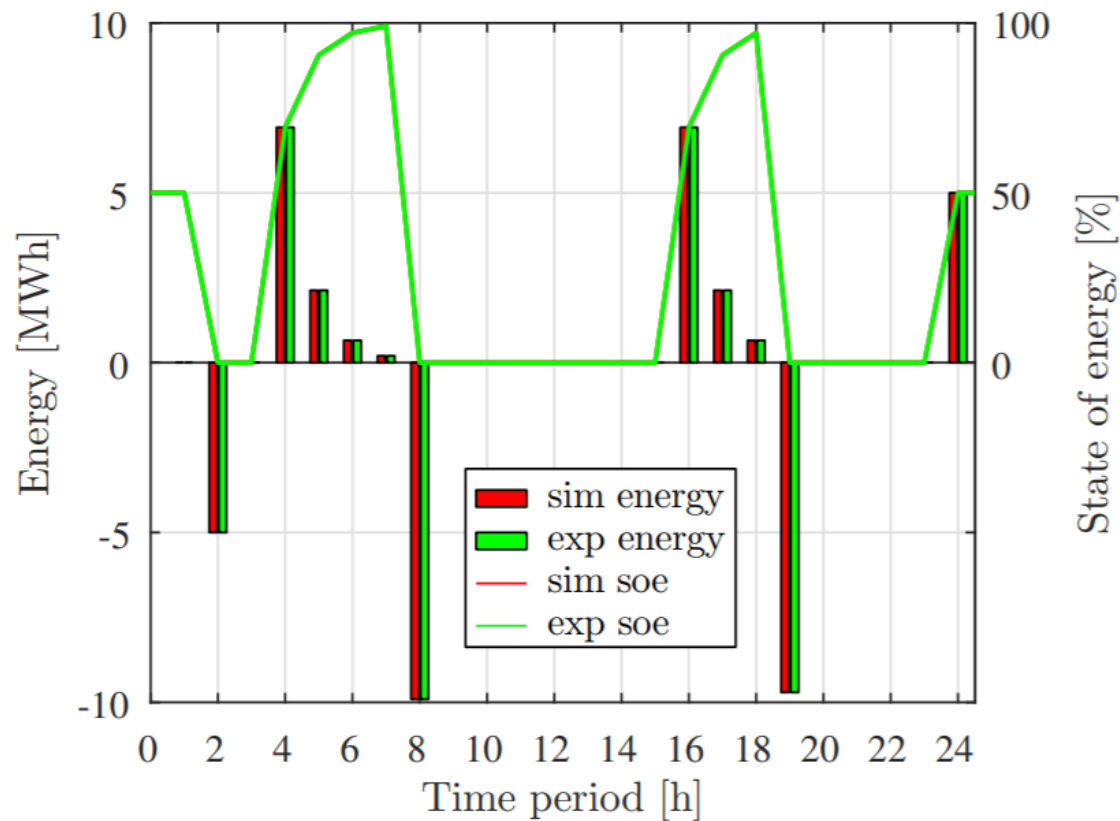
- The battery is considered to be at 50% state of energy at the beginning of the optimization horizon and is required to end up at that level
- Experimentally obtained overall battery energy efficiency (η) amounts to 0.81 for 1C simulations, and to 0.866 for 0.2C simulations

Results for 1C Rate



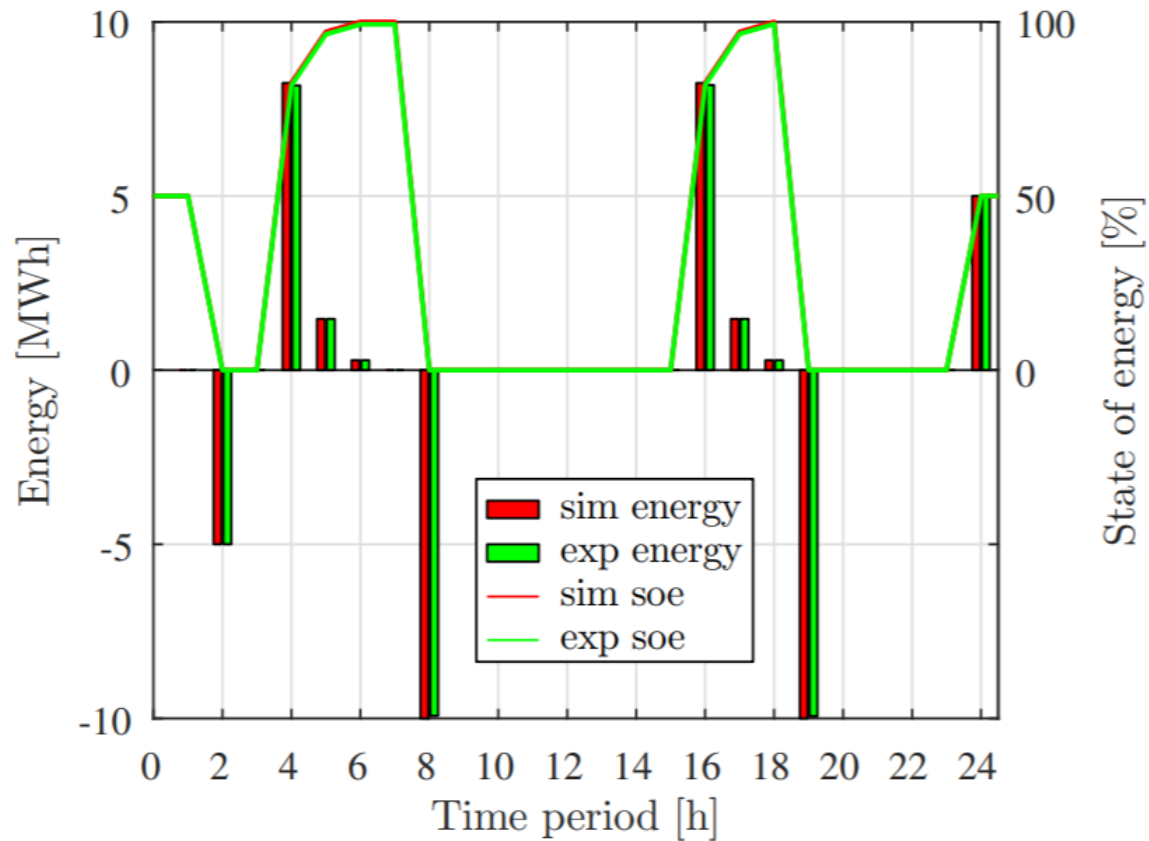
(a) Baseline model

Results for 1C Rate



(b) Linear CC-CV model

Results for 1C Rate



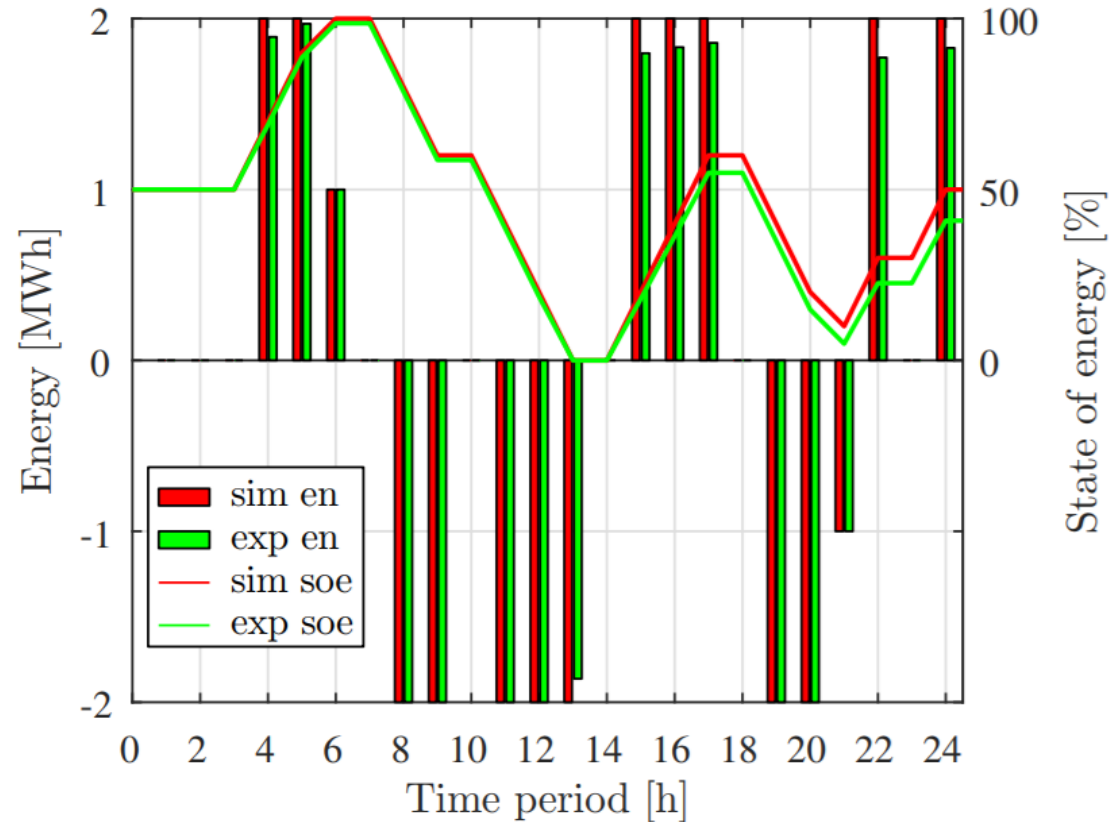
(c) Energy charging model

Results for 1C Rate

Model		Baseline	Linear CC-CV	Energy Charging
Delivered energy (MWh)	Simulation	25.00	24.62	25.00
	Experiment	21.41	24.62	24.87
Charged energy (MWh)	Experiment	21.41	24.62	24.87
Resulting profit (€)	Simulation	272.04	249.51	264.91
	Experiment	92.84	249.51	258.15

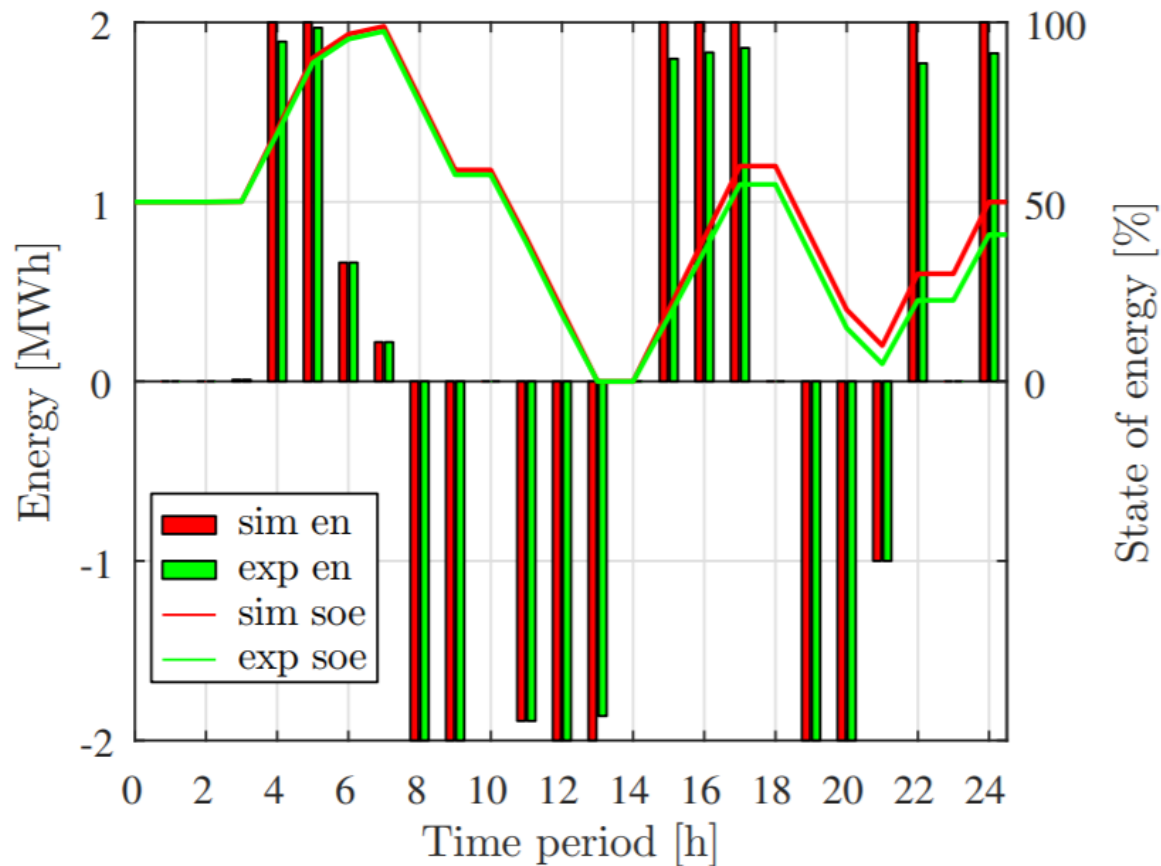
- ❑ If the charging quantity cannot be met, the electricity not charged is sold at 70% of the purchasing price
- ❑ If the discharging quantity cannot be met, the additional electricity is purchased at 140% of the day-ahead price

Results for 0,2C Rate



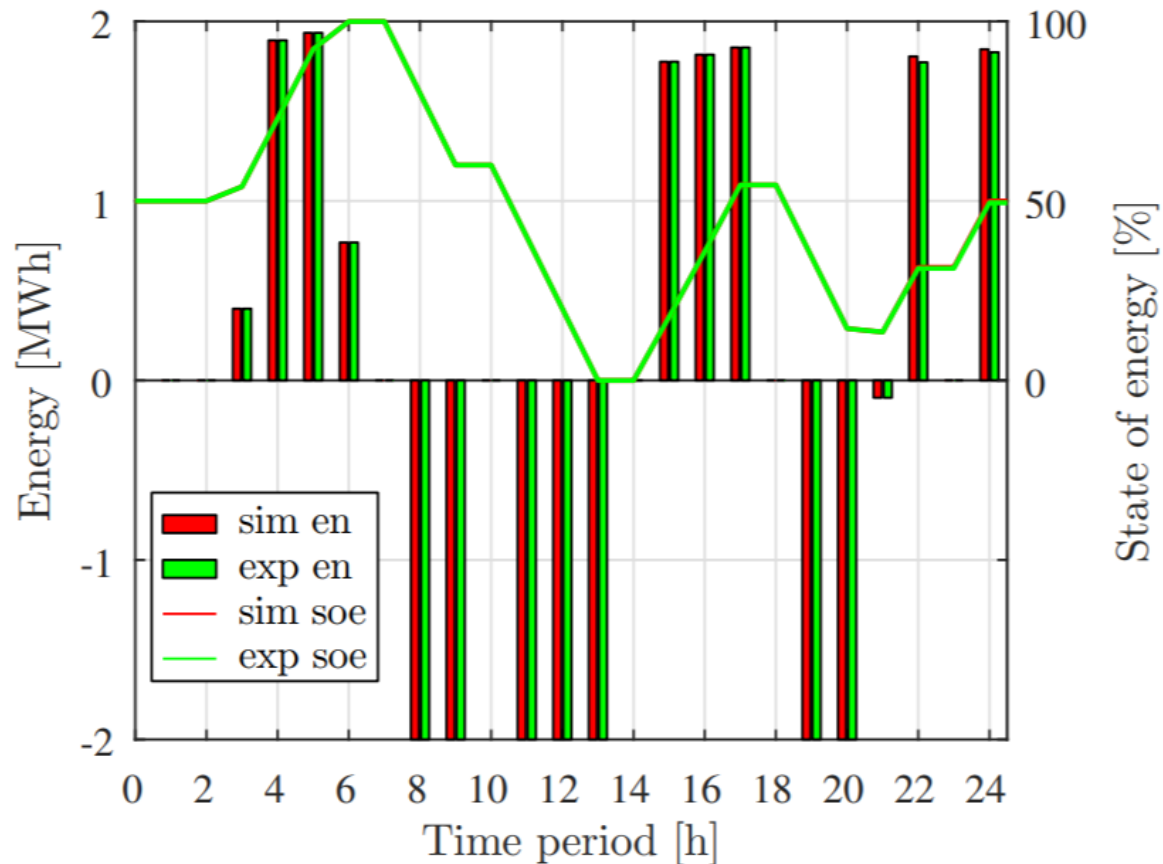
(a) Baseline model

Results for 0,2C Rate



(b) Linear CC-CV model

Results for 0,2C Rate



(c) Energy charging model

Results for 0,2C Rate

Model		Baseline	Linear CC-CV	Energy Charging
Delivered energy (MWh)	Simulation	15.00	14.89	14.10
	Experiment	14.86	14.76	14.10
Charged energy (MWh)	Experiment	13.95	13.84	14.05
Resulting profit (€)	Simulation	202.39	196.79	198.44
	Experiment	162.28	156.72	196.61

Conclusion

Procedure to obtain accurate dependency of the battery charging capacity on its state of energy:

1. record battery charging/discharging characteristic for the desired charging/discharging currents;
2. obtain charging/discharging energies by integrating the charging/discharging power in time;
3. determine battery capacity and overall energy efficiency;

Conclusion

Procedure to obtain accurate dependency of the battery charging capacity on its state of energy:

4. derive the time – soe curve from the charging energy characteristic;
5. derive soe – Δ soe curve from the time – soe curve;
6. approximate nonlinear soe– Δ soe curve by a piecewise linear function in order to obtain input parameters for the proposed model